Iron and copper on *Botrytis cinerea*: new inputs in the cellular characterization of their inhibitory effect

Fátima Rodríguez-Ramos[1], Vilbett Briones-Labarca[1], Verónica Plaza[2], Luis Castillo[2]

[1] Departamento de Ingeniería en Alimentos, Universidad de La Serena, La Serena, Coquimbo, Chile

[2] Departamento de Biología, Universidad de La Serena, La Serena, Coquimbo, Chile

Corresponding Author:
Luis Castillo[2]
Av. Raúl Bitrán Nachary 1305, Box 599, 1720010 La Serena, Chile.
Email address: lcastillo@userena.cl

Abstract

Certain metals play key roles in infection by the gray mold fungus, *Botrytis cinerea*. Among them, copper and iron are necessary for redox and catalytic activity of enzymes and metalloproteins, but at high concentrations they are toxic. Understanding the mechanism requires more cell characterization studies for developing new, targeted metal-based fungicides to control fungal diseases on food crops. This study aims to characterize the inhibitory effect of copper and iron on *B. cinerea* by evaluating mycelial growth, sensitivity to cell wall perturbing agents (congo red and calcofluor white), membrane integrity, adhesion, conidial germination, and virulence. Tests of copper over the range of 2 to 8 mM and iron at 2 to 20 mM revealed that the concentration capable of reducing mycelial growth by 50% (IC_{50}) was 2.87 mM and 9.08 mM for copper and iron, respectively. When mixed at equimolar amounts there was a significant inhibitory effect mostly attributable to copper. The effect of Cu_{50}, Fe_{50}, and Cu_{50}-Fe_{50} was also studied on the mycelial growth of three wild *B. cinerea* strains, which were more sensitive to metallic inhibitors. A significant inhibition of conidial germination was correlated with adhesion capacity, indicating potential usefulness in controlling disease at early stages of crop growth. Comparisons of the effects of disruptive agents on the cell wall showed that Cu, Fe, and Cu-Fe did not exert their antifungal effect on the cell wall of *B. cinerea*. However, a relevant effect was observed on plasma membrane integrity. The pathogenicity test confirmed that virulence was correlated with the individual presence of Cu and Fe. Our results represent an important contribution that could be used to formulate and test metal-based fungicides targeted at early prevention or control of *B. cinerea*.

Introduction

Botrytis cinerea is a phytopathogen of great interest in the agri-food field. As the second most critical fungal disease worldwide (Dean et al., 2012), and one that can affect a broad range of plant species (Kai et al., 2020), *B. cinerea* causes significant pre- and post-harvest losses, estimated at US$10-100 billion annually worldwide (Hua et al., 2018). It is capable of infecting more than 500 species of vascular plants (Spada et al., 2021), predominantly fruits and vegetables, affecting all organs: flowers, leaves, roots, and shoots (Torres-Ossandón et al., 2019). The main affected crops include vegetables such as tomato, zucchini, and cucumber, and fruit-bearing plants like grape, strawberry, and raspberry (Cheung et al., 2020).

Chemical fungicides are the most common biocides used to control *B. cinerea* (Castro et al., 2019; Nakajima & Akutsu, 2014). Hydroxyanilides, anilinopyrimidines, carboxamides, phenylpyrroles, and benzimidazole carbendazim are the fungicides widely used against this pathogen (Kai et al., 2020; Olea et al., 2019). They have diverse mechanisms of action. For example, fenhexamid inhibits the 3-ketoreductase involved in demethylation during ergosterol biosynthesis (Debieu et al., 2013), while boscalid is a succinate dehydrogenase inhibitor (Cherrad et al., 2018). Indiscriminate chemical use has resulted in the appearance of *Botrytis* strains resistant to a single fungicide or multiple fungicides. In addition, the fungicide compounds could cause harm to human health and the environment (Rupp et al., 2017). The numerous enzymes, metalloproteins, and metabolites produced by *B. cinerea* may play key roles in the infection and proliferation of the pathogen (Nakajima & Akutsu, 2014; Choquer et al., 2007). Transition metals provide the necessary redox and catalytic activity for various biological processes and may have direct or indirect roles in the pathogenicity of *B. cinerea* (Gerwien et al., 2018). These processes, require the ubiquitous presence of metal ions, such as Co, Cu, Mn, Fe, and Ni, as catalysts, structural elements in proteins, for electron transfer reactions, or as messengers (Antsotegi-Uskola, Markina-Iñarrairaegui & Ugalde, 2020). However, although metals are essential elements for growth and survival, both deprivation as well as metal overload is detrimental (Blatzer & Latgé 2017).

Copper and iron have been studied to elucidate their role in the virulence pathways of fungi (Antsotegi-Uskola, Markina-Iñarrairaegui & Ugalde, 2020; Gerwien et al., 2018). In the specific case of copper, two oxidation forms are usually present in the environment: Cu^{2+} and Cu^{+}, but only the form 1+ is recognized as a substrate by the transporters, since the extracellular Cu^{2+} is reduced via plasma membrane reductases prior to incorporation. Cu^{+} uses a passive transport to enter the cell, helped by an extremely low intracellular copper concentration (Balamurugan & Schaffner 2006). When the intracellular copper levels exceed the toxicity threshold in fungi, detoxification mechanisms are activated in order to reestablish cellular copper balance: the first mechanism is related to the chelation due copper sequestration by metallothionein's, and the second mechanism relies on PIB-type ATPases, which contain metal (Cu) binding domains rich in cysteine and histidine (Antsotegi-Uskola et al., 2020). In the case

78 of *B. cinerea*, copper-dependent proteins play an essential role in many aspects of virulence,
79 including pathogenesis and the copper detoxification system, as critical factors in the infection
80 mechanism (Saitoh and Izumitsu 2010; Smith et al., 2017).
81
82   Iron is an essential nutrient for all eukaryotes and almost all prokaryotes due to its
83 required metabolic function (Jhonson 2008). It has the most diverse roles in cellular processes,
84 especially in central metabolic pathways such as oxygen delivery and the electron transport
85 chain, primarily via incorporation of iron into the active centers of crucial enzymes, or in the
86 utilization of iron in siderophores (Gerwien et al., 2018). This metal is considered a fundamental
87 element for virulence in many microbial pathogens, including *B. cinerea* (Vásquez-Montaño et
88 al., 2020). Most fungi and bacteria exhibit specific mechanisms for the acquisition of iron from
89 the hosts they infect for their own survival, because iron is not easily available in the
90 environment due to host sequestration (Jhonson, 2008). In the case of fungi, four different
91 mechanisms have been identified: (1) ferric iron uptake mediated low- molecular-weight Fe (III)-
92 siderophores, which are non-ribosomally synthesized secreted iron chelators key in the uptake,
93 intracellular transport, and storage of iron (Haas, 2014); (2) reductive iron assimilation (RIA)
94 through a plasma membrane system; (3) low-affinity ferrous iron uptake and, (4) heme uptake
95 and degradation (Hass, H. 2014; Condon et al., 2014; Vásquez-Montaño et al., 2020). Most
96 fungal species employ more than one of these systems in parallel but rarely are all four strategies
97 present in the same specie (Haas et al 2008). Specifically, the siderophores have been considered
98 relevant not only for adaptation to iron starvation conditions or iron storage, but also for asexual
99 and sexual propagation, germination, resistant to oxidative stress, mutual interaction, protection
100 against iron-induced toxicity in some fungal organisms, microbial competition as well as
101 virulence in plant and animal hosts (Jhonson, 2008; Haas, 2014). High-affinity iron uptake
102 systems function during iron-limiting conditions, such as siderophore-mediated iron uptake and
103 reductive iron assimilation, enable fungi to acquire limited iron from animal or plant hosts,
104 whereas low-affinity systems are important during periods of relative iron abundance (Jhonson
105 2008), and include the iron-containing protein (e.g. heme, ferredoxin) uptake pathway and the
106 ferrous iron uptake pathway, where the siderophore-mediated iron uptake pathway is the most
107 extensively reported (Liu et al., 2020). Regarding *B. cinerea*, is expected to produce at least nine
108 siderophores, being ferrirhodin the main and the most abundant, but this pathogen can also take
109 up five other known siderophores, with the following order of uptake: ferrichrysin, ferrirubin,
110 ferrirhodin, hexahydroferrirhodin and, coprogen (Vásquez-Montaño et al., 2020; Konetschny-
111 Rapp et al., 1988).
112
113   As redox-active metals, the redox properties of iron and copper (variable oxidation states,
114 catalytic activity, complex formation, redox couples), are also responsible for the toxicity of
115 these elements when they are in excess because of the formation of highly reactive oxygen
116 species through the Fenton reaction. In addition, copper can displace iron in various proteins,
117 emphasizing the need for an optimal balance of these metals (Blatzer & Latgé 2017). Since

118   copper at high enough concentration is toxic to fungi, a variety of copper compounds has been
119   used through the years as antifungal agents in agriculture. Since the first use of copper in
120   vineyards in 1885, through the well-known Bordeaux mixture ($CuSO_4\cdot5H_2O + Ca(OH)_2$) for the
121   control of pathogenic fungi such as *Plasmopara viticola* and *B. cinerea* (Judet-Correia et al.,
122   2011), there has been an evolution in the development of antimicrobial formulations based on
123   copper for the protection of crops. Currently, there are several copper-based fungicides
124   commercially available: "Cobre premium" (copper oxide (I), 60 %) from Syngenta®;
125   Agrocopper ($CuSO_4\cdot5H_2O$, 98%) from Bayer®; and Captain Jacks® based on $C_{16}H_{30}CuO_4$ (10%)
126   from Bonide.
127
128   Judet-Correia et al. (2011) modeled the inhibitory effect of Cu on the growth of *B.*
129   *cinerea* (strains BC1 and BC2)*,* where the half-maximal inhibitory concentration (IC_{50}) was 2.21
130   and 2.60 mM, for the strains respectively, indicating that Cu may bind to the surface of the
131   spores during germination, requiring adequate time for a detoxification process and a subsequent
132   selection of surviving spores. In general, the mechanism of action of Cu in fungi has not been
133   entirely elucidated: low concentrations of this metal act as an essential nutrient facilitating its
134   proliferation, while higher concentrations are fungitoxic. Its toxicity is related to three relevant
135   effects: (1) delays in the germination of spores; (2) redox imbalance at the cellular level with
136   damage to membranes; and (3) inhibitory effects on the activity of the enzyme laccase,
137   preventing infection (Buddhika, Savocchia & Steel, 2020; Judet-Correia et al., 2011;
138   Lamichhane et al., 2018). Iron, which can exist as ferrous (Fe^{2+}) or ferric (Fe^{3+}) ions, is an
139   essential nutrient and necessary for the virulence of fungi that cause disease (Robinson et al.,
140   2021). Unlike Cu, Fe has been widely applied as a fertilizer. Since this metal is considered the
141   third most limiting nutrient for plant growth and metabolism and, its deficiency is a usual
142   nutritional disorder in many crops, resulting in poor yields and reduced nutritional quality (Rout
143   & Sahoo, 2015). Specifically, the use of iron as foliar fertilizer has often affected positively the
144   yields and quality of fruits and other crops, especially when levels of available soil nutrients are
145   low (Ma et al., 2019). However, various studies have evaluated its effect as an antifungal at
146   certain concentrations, because of the reported triggering at the cellular level of reactive oxygen
147   species via Fenton chemistry, resulting in oxidative damage to the microbes (Gerwien et al.,
148   2018; Touati, 2020). Studies have been done to assess the effect of Fe on *B. cinerea* and other
149   relevant phytopathogens in grape crops (Fleurat-Lessard et al., 2011), and 10 mM caused
150   dramatic changes in hyphal organization, favoring cell death, while no toxicity was observed on
151   grapevine leaves.
152
153   Previous evidence showed that iron and copper compounds could successfully inhibit mycelial
154   growth and conidial germination of *B. cinerea*. However, more studies are needed to expand our
155   understanding of the mechanisms of action at the cellular level for this critically important
156   pathogen. Thus, this study aimed to deliver new contributions in this area by characterizing the

157   antifungal effect of copper, iron, and their mixture on *B. cinerea*, evaluating membrane integrity,
158   cell wall alteration, adhesion capacity, conidial germination, and pathogenicity.
159

Materials & Methods

161

Fungal strains and growth conditions

163

164   The *B. cinerea* reference strain B05.10, a haploid wild-type strain originally isolated from grapes
165   (Biittner et al., 1994; Quidde et al., 1998) is available from the International Collection of
166   Microorganisms from Plants (New Zealand, Strain no. ICMP 17.435). The three wild strains
167   studied (Bc.po03, Bc. vi09, and Bc. ad03) were isolated from different plants and locations in
168   Coquimbo Region, Chile (unpublished data) (See **Table S1**). *B. cinerea* strains were grown on
169   potato dextrose agar (PDA, Difco™), malt extract broth (MEB), and malt extract agar (MEA,
170   2% malt extract and 2% agar, Merck). MEA plates were inoculated with 10 µL of conidial
171   suspension (2.5×10^5 conidia/mL) and cultured for 12 days at 25°C under a photoperiod of 12 h
172   light/12 h darkness in a Percival incubator (Percival, USA) followed by 10 days of total
173   darkness. Sporulating cultures were washed with sterile water and filtered (Plaza et al., 2015).
174

DNA Extraction, PCR Amplification and Sequencing

176

177   Genomic DNA extraction was performed as in a previous publication according Notte et al.
178   (2021) and it was using standard protocols (Sambrook, Fritsch & Maniatis, 1989). The DNA
179   pellets were dissolved in 50µL of TE buffer (10mM Tris-HCl [pH 8.0], 1mM EDTA) and
180   quantified using a Nanodrop spectrophotometer. To identify *B. cinerea* species we sequenced the
181   ITS region and glyceraldehyde-3-phosphate dehydrogenase (G3PDH), Heat-shock Protein 60
182   (HSP60), DNA-dependent RNA polymerase subunit II (RPB2) and protein encoding necrosis
183   and ethylene inducing protein 1 (NEP1) genes (Staats et al., 2005; White et al., 1990). Primer
184   pairs (Table S2) were designed to amplify the *G3PDH*, *HSP60*, *RPB2* and *NEP1* genes. For
185   amplifications of ITS region, primers IST1 and ITS4 were used (White et al., 1990). The PCR
186   reaction and the thermocycling pattern to amplify *HSP60, G3PDH,* NEP1 and *RPB2* were
187   following according to Notte et al. (2021) and Staats et al. (2005). The presence of transposons
188   was detected by PCR with the primers boty-F and boty-R to amplify boty transposon, and the
189   primers F300 and F1500 to detect the flipper transposon (**Table S2**) according to Giraud et al.
190   (1999) and Muñoz et al. (2010), respectively.
191

Molecular and phylogenetic identification

193

194   For the identification of native isolates *Botrytis* sp., analysis of *HSP60*, *RPB2*, *G3PDH* and
195   *NEP1* genes were sequenced using the same primers by Macrogen (Seoul, Korea). The multiple
196   alignments were performed using CLUSTAL W (Thompson, Higgins & Gibson, 1994). The

197 phylogenetic trees were constructed based on the neighbor-joining method (Saitou N, 1987) and,
198 the topology confirmed with the Maximum Likelihood and Maximum Parsimony methods by
199 using the MEGA X software (Kumar et al., 2018). Distance matrices were calculated by the
200 Kimura 2-parameter method and bootstrap analysis was performed based on 1000 re-samplings
201 (Kumar et al., 2018). Nucleotide sequences of *HSP60*, *RPB2*, *G3PDH* and *NEP1*, commonly
202 used for differentiation of *Botrytis* species, were obtained from the GenBank website and
203 compared with the partial sequences of the HSP60 (705 bp), RPB2 (924 bp), G3PDH (690 bp)
204 and NEP1 (336 bp) genes from native isolates (Bc.ad03, Bc.po03 and Bc.vi09) (Table 4).
205
206 **Effect of Cu, Fe, and Cu-Fe on mycelial growth of B05.10 and wild strains of *B. cinerea***
207
208 The effect of copper and iron on the mycelial growth of B05.10 was measured using the radial
209 growth test on PDA (pH 5.40). The methodology was based on a modified version of the
210 protocol developed by Judet-Correia et al. (2011) and Fleurat-Lessard et al. (2011). Stock
211 solutions of Cu (100 mM [pH 2.01]), and Fe (200 mM [pH 2.34]) ($CuSO_4 \cdot 5H_2O$ and
212 $FeSO_4 \cdot 7H_2O$, Merck) in sterile water were prepared, filtered through an MF-Millipore™
213 membrane filter (0.22 µm pore size), and diluted to obtain a range of final concentrations in
214 medium (Cu: 2, 4, 6, 8 mM; Fe:2, 4, 6, 8, 10, 12, 14, 20 mM; and equimolar mixture of Cu-Fe: 2,
215 4, 6, 8, and 12 mM). The medium was poured into 90 mm diameter Petri dishes, which were
216 inoculated with 10 µL of conidial suspension (1×10^6 conidia/mL) and incubated at 25°C in the
217 dark for seven days. Mycelial growth diameters were measured daily using a caliper, and the
218 inhibition values were calculated. IC_{50} values for B05.10 mycelial growth were estimated at day
219 7 of incubation and analyzed by linear regression using the software GraphPad Prism (version
220 9.2.1). All experiments were performed with n = 6 samples and the results were expressed as
221 means ± SD. The same procedure previously described, was used to measure the effects of metal
222 inhibitors on the mycelial growth of three wild strains of *B. cinerea* (**Table S1**) for 6 days*, but
223 considering the IC_{50} values estimated previously, and the inhibition rate was compared with the
224 B05.10 strain.
225
226 The inhibitory effect on *B. cinerea* (B05.10 and wild strains) was also studied in the
227 presence of mixtures based on metallic inhibitors Cu (IC_{50} 2.87 mM) and Fe (IC_{50} 9.08 mM),
228 with commercial fungicides (12.8 ppm boscalid, 4.8 ppm iprodione, and 15.35 ppm fenhexamid)
229 in terms of the survival rate (%). For this purpose, a preliminary analysis of chemical
230 compatibility in terms of solubility was initially performed for the antifungal-metal mixtures to
231 define the antifungals to be studied. The assay was conducted in 96-well plates using MEB
232 medium, considering the study of the mixtures and controls: antifungals, metals, and strains
233 under study. In each well, a total of 100 µL of each variant to be evaluated was added, followed
234 by 100 µL of conidial suspensions (2.5×10^5 conidia/mL) and incubated at 25°C for 72 hours, for
235 a total volume of 200 µl, ensuring the desired concentrations to be evaluated. Finally, the
236 absorbance at 600 nm was measured with an Epoch microplate spectrophotometer (BioTek

237 Instruments, USA). The optical density (OD) values were proportional to the quantity of biofilm
238 formed, comprising mycelium and extracellular polymeric material. Results for the OD were
239 compared with the control to estimate the survival rate of the variants studied. The synergism
240 pattern among the components of mixtures was determined according to the mixture index (MI)
241 expression (Giovagnoli-Vicuña et al, 2019):

242
$$MI = \frac{AC_1C_2}{AC_1 + AC_2}$$

243 where, AC_1C_2 was the value of inhibition percentage (%) for mixtures and (AC1 +AC2) was the
244 value obtained by the sum of % inhibition for each individual inhibitor (antifungal or metal). The
245 following cutoff values were chosen, for the interpretation of obtained results: synergism MI is
246 >1, MI= 1 addition, and MI< 1 would be antagonism.
247
248 **Effect of Cu, Fe, and Cu-Fe on adhesion capacity of B05.10.**
249
250 The adhesion capacity of *B. cinerea* was measured in the presence of Cu_{50}, Fe_{50}, and the mixture
251 (Cu_{50}-Fe_{50}) to determine their effect on this parameter. The methodology used was based on a
252 modified version of the protocol developed by Plaza et al. (2015). First, aliquots of 100 µL of
253 2.5×10^5 conidia/mL were added to sterile polystyrene 96-well microtiter plates (JetBiofil,
254 China). Then, 200 µL of Malt Extract Broth (2% Malt) (MEB, pH 4.70) containing the
255 concentrations of Cu_{50} (pH 3.45), Fe_{50} (pH 3.88), and Cu_{50}-Fe_{50} (pH 3.33) were added to reach
256 the IC_{50} values in each well. Plates were incubated in darkness at 25°C for five days, then the
257 medium containing unbound conidia was aspirated, and remaining non-adherent conidia were
258 removed by washing three times with 250 µL sterile water. Next, 100 µL of 0.1% methyl violet
259 in glacial acetic acid was added to the adherent cells and allowed to stain for 5 min. The wells
260 were washed three times with 250 µL of phosphate-buffered saline (PBS) and absorbance at 590
261 nm was measured with an Epoch microplate spectrophotometer (BioTek Instruments, USA). The
262 optical density (OD) values were proportional to the quantity of biofilm formed, comprising
263 mycelium and extracellular polymeric material.
264
265 **Effect of Cu, Fe, and Cu-Fe on conidial germination of B05.10.**
266
267 The effect on conidial germination of *B. cinerea* in the presence of Cu_{50}, Fe_{50}, or Cu_{50}-Fe_{50} was
268 determined according to the methodology of Torres-Ossandón et al. (2019). Briefly, 500 µL of
269 an aqueous suspension of 2.5×10^5 conidia/mL and aliquots of inhibitors were combined and the
270 volume made up to 1.0 mL with MEB medium, and incubated at 22°C using constant agitation
271 for 0, 4, and 6 h. Afterwards, the conidia were collected by centrifugation at 13.680 xg for 5
272 minutes and washed twice with 500 µL of sterile water. The pellet was resuspended in 100 µL of
273 sterile water and 10 µL aliquots of each sample were placed on slides, cover-slipped, and
274 examined under a light microscope (Eclipse E-200, Japan). The percentage (%) of germinated
275 conidia was assessed on microphotographs of the images. As a rule, the conidia were considered

276   germinated when the length of the germ tube was twice the length of the conidia (Torres-
277   Ossandón et al., 2019). Three replicates were evaluated for each treatment, and a minimum of
278   100 conidia was counted for each replicate.
279
280   **Membrane integrity assay**
281
282   The effect on *B. cinerea* membrane integrity in the presence of Cu_{50}, $Fe_{50,}$ and Cu_{50}-Fe_{50} was
283   determined according to the methodology of Torres-Ossandón et al. (2019). Aqueous
284   suspensions of 5×10^5 conidia/mL untreated and treated with inhibitors in MEB medium (final
285   volume of 1 mL) were incubated in a shaker at 22°C for 4 and 6 h. Afterwards, the conidia were
286   collected by centrifugation at 3.465 xg for 10 min/25°C, washed twice with 500 μL of 50 mM
287   sodium phosphate buffer (pH 7.0), and centrifuged at 13.680 xg for 2 min. The conidia were then
288   stained with 1 mL of 10 μg/mL propidium iodide (PI) for 5 min at 30°C with incubation at 30°C
289   in a digital dry bath (Accu Block, D1200, NJ, USA). Lastly, conidia were collected by
290   centrifugation at 13.680 xg for 2 min, washed twice with buffer to remove residual dye, and
291   observed under a light microscope with an epifluorescence system (Eclipse E-200, 400X, Japan).
292
293   **Sensitivity to cell wall perturbing agents**
294
295   Congo red (CR) and calcofluor white (CFW) were evaluated as cell wall stressing agents in
296   terms of the sensitivity of *B. cinerea*. For this assay, the methodology used was from Plaza et al.
297   (2015), with some modifications. Initially, 500 μL of aqueous suspensions of 2.5×10^5
298   conidia/mL were pre-incubated in MEB medium with 500 μL of inhibitors (Cu_{50}, Fe_{50}, and Cu_{50}-
299   Fe_{50}) for 4h with agitation at 22°C. Then, 20 μL aliquots of each preparation were inoculated into
300   growing medium, previously prepared with 2% MEA, and 500 μg/mL each of CR, and CFW in
301   90 mm diameter Petri dishes. Samples were incubated in darkness at 22°C for six days, and
302   mycelial growth diameters were measured daily. All experiments were performed with $n = 9$
303   samples.
304
305   **Pathogenicity test**
306
307   To assess the pathogenicity of *B. cinerea* in the presence of inhibitors (Cu_{50} and Fe_{50}), a test was
308   performed on strawberry fruits (*Fragaria ananassa*) and tomato leaves (*Solanum lycopersicum*).
309   The methodology of Doehlemann et al. (2006) and Plaza et al. (2015) was used with some
310   modifications. Before inoculation, the strawberry tissues and detached leaves of tomato were
311   wounded with a pinprick of a 21G syringe and surface-sterilized by immersion with 75% ethanol
312   for 1 min. For inoculation, 5 μL of 2.5×10^5 conidia/mL suspensions were used with a subsequent
313   incubation step at 25 °C. The lesion diameters were measured using a Caliper up to 4 days after
314   inoculation. Strawberry fruit tests were performed with n = 15 samples and n =10 for detached
315   tomato leaves.

316 **Statistical analysis**

317

318 The Statistical analysis was carried out according to the protocol of Leiva-Portilla et al. (2020).
319 A One-way Analysis of Variance (ANOVA) was selected to evaluate significant differences
320 considering p-value < 0.05 between the means, using Statgraphics Centurion XVI (Statistical
321 Graphics Co., Rockville, MD, USA). Additionally, the Least Significant Difference (LSD) test
322 was used to examine the differences among the media based on a confidence interval of 95%,
323 while the presence of homogeneous groups within each parameter, was validated by the Multiple
324 Range Test (MRT). All the experiments were conducted at least three times.

325

326 # Results

327

328 **Effect of Cu and Fe on *B. cinerea* mycelial growth on solid media**

329

330 The antifungal activity of Cu and Fe and their equimolar mixture was assessed against the *B.*
331 *cinerea* B05.10 strain based on mycelial growth inhibition. For Cu, the concentration range
332 studied was 2-8 mM (**Fig. 1A**). The results indicated that concentrations greater than 4 mM
333 effectively inhibited the mycelial growth of *B. cinerea* by 85 to 94%, while 2 mM resulted in
334 almost 8% inhibition, after seven days of growth. However, for iron, concentrations between 2
335 and 20 mM were tested for mycelial growth inhibition (**Fig. 1B**). At 2-4 mM, no inhibitory effect
336 was observed, since the mycelial growth pattern was similar to the control. In contrast, 6, 8, and
337 10 mM inhibited the fungus by 6, 29, and 56%, respectively. The results showed that the IC_{50} for
338 iron capable of reducing 50% growth on solid media was equal to 9.08 mM.

339

340 Results for the effect of equimolar concentrations of Cu and Fe on the growth of *B. cinerea*
341 B05.10 strain are depicted in **Fig. 2.** The Cu-Fe mixture at 2 mM showed a low inhibition near
342 the control level, corroborating the findings for Fe and Cu applied individually. An interesting
343 effect was observed for 4 mM of Cu-Fe, which resulted in nearly 75% inhibition of mycelial
344 growth. The toxic concentration for Cu alone resulted in inhibition of 85%, while for iron, the
345 inhibition was not significant. Cu appears to have the predominant inhibitory effect on mycelial
346 growth in this equimolar mixture in comparison to Fe with a minimum contribution **(Fig. 2A, B).**
347 Figure S1 depicts the effect of Cu, Fe, and Cu-Fe on radial growth rate. In the presence of Fe, the
348 radial growth rate was constant in the range 0-4 mM. From 4 mM to 12 mM, there was a
349 continuing decrease until the rate leveled off at 14 mM with a radial growth rate average equal to
350 0.78 mm/day. In the case of Cu, the decay rate was more drastic from 2 mM until 8 mM,
351 evincing a superior fungitoxicity on B05.10. At the same time, Cu-Fe showed an effect similar to
352 that of Cu alone on radial growth rate from 2 mM, with a subsequent constant decrease until 12
353 mM, corroborating the predominant effect of Cu in inhibiting mycelial growth in B05.10.

354

355

Antifungal response of wild strains of *B. cinerea* to treatment with metal inhibitors and metal-fungicides mixtures

To test for possible resistance or different sensitivity patterns, the effects of Cu_{50} and Fe_{50}, and the Cu_{50}-Fe_{50} mixture were assessed on mycelial growth of the three wild strains: Bc.po03, Bc.vi09 and, Bc.ad03, which have been shown to have different patterns of sensitivity and resistance to specific concentrations of commercial antifungals **(Table S3).** To determine their identity, all isolates were subjected to DNA sequence analysis (ITS analysis and nuclear protein-coding genes were sequenced) **(Table S4)**, and the procedure was based on a previous work (Notte et al., 2021). The partial sequences of the *HSP60* (705 bp), *RPB2* (924 bp), *G3PDH* (690 bp) and *NEP1* (336 bp) genes analyzed by BLAST report a high percentage of identity of all isolates obtained with strains and isolates of *B. cinerea* **(Table S5).** Therefore, based on these results, the phylogenetic position observed by concatenated genes (*G3PDH*, *HSP60*, *RPB2* and *NEP1*) groups all isolates obtained in a single clade together with *B. cinerea* B05.10 **(Fig. S2).**

Results showed that the wild strains were sensitive to the tested concentrations of Cu_{50}, Fe_{50}, and Cu_{50}-Fe_{50} **(Fig. 3)**. For Bc.po03, isolated from *Porlieria chilensis*, Cu_{50} inhibited 78.05 % of the mycelial growth by day 2, compared to control. There was a continuing decrease until day 6, when the metal treatments reached a maximum inhibition of 85.46%. A similar trend with Cu_{50} was observed for the other wild strains, being more marked for Bc.ad03 with a final inhibition of 78.41% (day 6), while Bc.vi09 from *Vitis vinifera* was the most sensitive strain, with a final inhibition of 88.57 % (day 6). Wild strains showed greater sensitivity to Fe_{50} than Cu_{50}, with a final inhibition greater than 92% in all cases. The inhibitory effect of Cu_{50}-Fe_{50} was not significantly different compared to iron alone for Bc.ad03 ($p = 0.05$), Bc.po03 ($p = 0.07$), and Bc.vi09 ($p = 0.73$). These strains were more sensitive to the Cu-Fe mixture than to Cu alone, and we conclude that iron has a dominant effect over copper. In addition, the wild strains were more sensitive to Cu_{50} and Fe_{50} in comparation to B05.10, however these strains displayed sensitivity similar to the effect caused by Cu_{50}-Fe_{50} mixture in B05.10.

Results for the effect on *B. cinerea* regarding mixtures of commercial fungicides-metal inhibitors **(Fig. S3)**, showed that on B05.10 the Cu-fungicides mixture (boscalid and fenexhamid) exhibited a synergistic effect with MI=1.2 in both cases, but for Cu-iprodione was antagonist (with iM<1); meanwhile on wild strains, the effect was also antagonist predominately. In the case of the mixtures with Fe, an antagonist effect was observed on B05.10 and Bc. vi09, whereas on other wild strains, the depicted effect had a more heterogeneous behavior, only boscalid-Fe on Bc. po03 showed a synergistic effect, while iprodione-Fe on Bc. po03 and Bc.ad03 were the only ones that showed an antagonist effect **(Table S6)**. The observed effects for all the metal-fungicides mixtures could be correlated considering the individual action mode on *B. cinerea* and, the resistance or sensitivity pattern displayed against boscalid, iprodione and fenexhamid by the studied strains.

Effect of Fe, Cu, and Cu-Fe on conidial germination

The effect on conidial germination of *B. cinerea* in the presence of Cu_{50}, Fe_{50}, and Cu_{50}-Fe_{50} was also determined. B05.10 without metallic inhibitors (**Fig. 4A**) revealed a regular pattern of conidial germination over the experimental time period, reaching 44% germination. In the presence of metallic inhibitors, significant inhibition of germination was seen at 4 and 6 h (**Fig. 4B**). The average percent conidial germination in the presence of Cu or Cu-Fe at 6 h was 6.36 ± 1.68 and 6.30 ± 1.60 %, respectively, with no significant difference between the two. In contrast, Fe showed an inhibition equal to 5.61 ± 1.61 %, and slightly lower than Cu and Cu-Fe.

Effect of Cu, Fe, and Cu-Fe on adhesion capacity of *B. cinerea*

The effect of metallic inhibitors on adhesion capacity was also evaluated (**Fig. 5A, B**). In the presence of Cu_{50}, B05.10 showed the lowest adhesion (0.9%) compared to the other inhibitors, with statistically significant differences (Cu versus Fe: $p = 0.0208$; Cu versus Cu-Fe: $p = 0.0170$, 95%). In the images of stained conidial tissue, remains of conidia with low germination were seen. However, Fe_{50} and Cu_{50}-Fe_{50} showed slightly higher adhesion compared to Cu (3%), but this difference was not statistically significant ($p = 0.8509$, 95%).

Effect of Fe, Cu, and Cu-Fe on cell wall and membrane integrity

Copper and iron are essential micro-nutrients, however, both can also be toxic in cells due to their redox properties and affecting the plasma membrane. The cell wall is a barrier that could help the cell to survive (Ghaed, Shirazi & Marandi, 2013; Tobin, White & Gadd, 1994). Therefore, the effect of Fe_{50}, Cu_{50}, and Cu_{50}-Fe_{50} on integrity of the cell wall of B05.10 was also analyzed. Conidia treated with metallic inhibitors were examined for their sensitivity to antifungal drugs that specifically affected cell wall assembly or the synthesis of its structural components (**Fig. 6 and 7**). Congo red affects microfibrils of β 1,3-glucans, and calcofluor white alters the assembly of chitin fibrils (Plaza et al., 2015; Torres-Ossandón et al., 2019). When the effects of Cu_{50}, Fe_{50}, and Cu_{50}-Fe_{50} were compared to the Congo red curves, there was some overlap where minimal alterations and effects on the cell wall were observed (**Fig. 6**). Some differences in the curves, such as the activity exhibited by Cu on day 5, were not statistically significant ($p = 0.44$, 95%). Evaluating CFW as a disturbing agent (**Fig. 7**), we found that its effect on B05.10 without inhibitors was lower than the effect of CR without inhibitors. In contrast, CFW treatment with inhibitors revealed that the effect on the cell wall was not due to the metals, which overlapped, but only with non-significant statistical differences.

The effects of Cu_{50}, Fe_{50}, and Cu_{50}-Fe_{50} on membrane integrity of *B. cinerea* were also studied using PI as a fluorescent indicator of *cell* viability. Untreated conidia and conidia treated with inhibitors for various times were stained with PI and imaged by fluorescence microscopy

436 (**Fig. 8A, B**). The effect of Fe and Cu on the membrane ranged from 2 to 6% at 0 h. The Cu-Fe
437 combination exerted an effect close to 20%. Effects on the membrane were more significant as
438 time progressed to 6 h, where conidia treated with Cu, Fe, and Cu-Fe showed damage to
439 membranes in 20.5, 15.51, and 30.85% of samples, respectively. The results suggested that the
440 mixture of these metals possibly exerted a synergistic effect in damaging the cell membranes of
441 *B. cinerea*, exhibiting a higher number of nonviable conidia.
442
443 **Pathogenicity test**
444
445 The pathogenicity patterns of B05.10 in the presence of Fe_{50} and Cu_{50} were also assessed as
446 performed on strawberry fruits and tomato leaves (**Fig. 9**). The growth of *B. cinerea* in the fruits
447 was measured on days 0 and 4 after inoculation. The results suggest that metal inhibitors were
448 able to inhibit mycelia growth after inoculation in wounds on the fruits, indicating the antifungal
449 effect at 2.87 mM and 9.08 mM for copper and iron, respectively. Regarding fruit senescence,
450 the comparison of fruit appearance from day 0 to 4 showed only minor changes with copper
451 compared to strawberries inoculated in the presence of iron. Regarding the test performed on
452 tomato leaves with metal inhibitors, after 4 days of incubation iron was able to inhibit mycelial
453 growth by 53.8% compared to B05.10, while copper inhibited to a lesser extent with 25.9%.
454
455
456 # Discussion
457
458   In this work, the results demonstrate that Cu, Fe, and Cu-Fe exhibit antifungal activity
459 against *B. cinerea* B05.10, grown on solid and liquid media. The effect of copper on mycelial
460 growth showed that a concentration of 2 mM was minimally toxic to the B05.10 strain. This can
461 be explained because the Cu requirements of microorganisms are usually satisfied with low
462 concentrations of this metal, on the order of l-10 μM, which serves as a micronutrient for the
463 growth and proliferation of filamentous fungi (Cervantes & Gutierrez-Corona, 1994). A similar
464 effect was observed by Buddhika, Savocchia & Steel. (2020) who showed that Cu^{2+} stimulated
465 growth of *B. cinerea* at concentrations below 0.6 mM. At concentrations greater than 2 mM,
466 especially between 4-8 mM, copper inhibited the mycelial growth of *B. cinerea*, with an IC_{50} of
467 2.87 mM. This value was comparable to those reported by Judet-Correia et al. (2011) on two
468 isolated strains of *B. cinerea* (BC1 and BC2) with IC_{50} values equal to 2.60 and 2.21 mM,
469 respectively. It has been reported that Cu can be highly toxic to microbial cells when present at
470 high levels in its free ionic form, Cu^{2+}. This effect is mainly related to its interaction with nucleic
471 acids, the oxidation of membrane components, and the modification of enzyme active sites
472 (Cervantes & Gutierrez-Corona, 1994). Accordingly, these processes can be linked to the
473 capacity of copper to produce toxic hydroxyl free radicals, generating redox imbalance at the
474 cellular level. These effects could explain the results found in our study where high
475 concentrations of copper affected mycelium growth in this fungus (Cervantes & Gutierrez-

476   Corona, 1994; Lamichhane et al., 2018). In addition, laccases are inducible enzymes produced by
477   filamentous fungi during the colonization of host plant tissues, and their activity is inhibited by
478   excess Cu, which prevents the infection (Schouten et al., 2002; Buddhika, Savocchia & Steel,
479   2020; Hernández-Monjaraz et al., 2018). Other authors showed evidence that copper toxicity in
480   fungi could occur because copper displaced essential metal cofactors from their native protein
481   binding sites or blocked ligand interactions (Borkow & Gabbay, 2005).
482
483   With regard to iron, it is an essential element for most organisms and a critical factor for fungal
484   virulence in pathogenic species (Gerwien et al., 2018; Liu et al., 2020). Its role is important as a
485   vital component of iron-sulfur clusters required for activation of nuclear proteins involved in
486   DNA repair (Robinson et al., 2021). Our data show that low iron concentrations in the range of
487   2-4 mM did not affect the growth of *B. cinerea*. However, iron concentrations greater than 4 mM
488   progressively inhibited the fungus, reaching a value of 56% for 10 mM, with inhibition
489   percentages near 93 % for 12-20 mM. The inhibition pattern obtained for iron, was compared
490   with data from Fleurat-Lessard et al. (2011) for *B. cinerea* (strains Bc 112 T, Bc 162 V, Bc 344
491   T, Bc 916 T), showing that the mycelial growth was not significantly affected by 1 mM, but
492   there was a strong effect at 10 mM and complete inhibition at 20 mM. A IC_{50} value for iron of
493   9.08 mM was determined, a value higher than the IC_{50} of Cu. This result could be explained by
494   one of the most plausible mechanisms, where fungitoxicity has been associated with redox
495   cycling between the ferric and ferrous forms, catalyzing the generation of dangerous free radicals
496   that are toxic to plants and pathogen cells (Liu et al., 2020). Iron homeostasis is therefore tightly
497   regulated (Greenshields, Liu & Wei, 2007). To maintain Fe homeostasis, fungi have to balance
498   Fe acquisition, storage, and utilization to guarantee an adequate supply and avoid a toxic excess
499   (Misslinger et al., 2021). Preserving the suitable balance of Fe between deficiency and toxicity
500   requires fine-tuned control of iron uptake and storage (Haas et al., 2008). According to Gerwien
501   et al. (2018), several pathogens have evolved elaborate systems to acquire iron from their
502   environment and to store the excess at a high concentration in a nontoxic form for times of need.
503   This could partly explain the tolerance observed for iron at concentrations between 4 and 6 mM
504   in our experiments.
505
506   A combination treatment of equimolar concentrations of Cu and Fe was also assessed on the
507   *B. cinerea* B05.10 strain. Significant antifungal activity of Cu-Fe at 4 mM or higher was
508   evidenced in comparison to the individual effects Cu or Fe. Interestingly, the *B. cinerea* cells
509   exhibited a high sensitivity to low concentrations of Cu as described before, but a possible
510   synergistic effect with Fe at concentrations greater than 4 mM. Our results are consistent with
511   other authors who have established that copper is highly toxic towards various microorganisms
512   including bacteria, yeasts, *Plasmopara viticola,* and *B. cinerea* (Judet-Correia et al., 2011;
513   Zoroddu et al., 1996). According to Gerwien et al. (2018), several common biological metals
514   have similar divalent cation properties in binding ligands but different catalytic functions. For
515   example, host-induced metal excess and oxidative stress can result in 'mismetallation', replacing

516 the normal metal cofactor of an enzyme with a different metal. This process inhibits the role of
517 microbial enzymes that require specific metals as cofactors (Imlay, 2014). In the case of copper,
518 some of its toxic effects arise from the high capacity of Cu^+ under anaerobic reducing conditions,
519 to displace other metals from their coordination sites, while, Cu^{2+} forms the most stable
520 complexes of the divalent transition metals (Gerwien et al., 2018; Irving & Williams, 1948).
521 Similar to copper, iron has a strong propensity for replacing other metals in reactive enzymatic
522 centers, which generally disrupts the enzyme function (Martin and Imlay, 2011; Vance and
523 Miller, 1998), generating an imbalance in the homeostasis of these metals. This could explain the
524 apparent synergistic effect between Cu and Fe on *B. cinerea*.

526   The effect of Cu, Fe, and Cu-Fe on mycelial growth *B. cinerea* B05.10 strain was
527 additionally compared with the effect of this pathogen on wild strains, showing that these strains
528 were more sensitive to the test concentrations of metallic inhibitors than B05.10. At the same
529 time, with the mixture of metallic inhibitors, wild strains displayed sensitivity similar to the
530 effect caused by iron, confirming the dominant effect of this metal. A similar antifungal pattern
531 was reported by Notte et al. (2021) for the diverse phenotypes and genotypes of the *B. cinerea*
532 isolates studied. It is important also to consider that diverse *B. cinerea* isolates displayed
533 different degrees of virulence and response to antifungal agents, which could be related to
534 intraspecific differentiation and different degrees of host adaptation of this pathogen (Plesken et
535 al., 2021). In addition, it has been reported that, some genes in *B. cinerea* that are important for
536 virulence, may contribute differently depending on the genetic background (Pinedo et al., 2009;
537 Siewers et al., 2005).

539   On the other hand, when metal-fungicides were evaluated, the synergistic effect
540 observed on B05.10 by the Cu-antifungal mixture could be associated with the disruptive effect
541 exerted by copper on the cell membrane in *B. cinerea* and, the mode of action of the fungicides.
542 For example, in the case of fenexhamid and boscalid, it has been reported that they interfere with
543 the biosynthesis of ergosterol (Debieu et al., 2013; Pappas and Fisher, 1978), a key component in
544 the architecture of the cell membrane, affecting its production and therefore the growth of the
545 fungus. While, in the case of boscalid, it is a succinate dehydrogenase inhibitor, affecting the
546 proper functioning of cellular metabolism (Cherrad et al., 2018; Piqueras et al., 2014). Then,
547 possibly, in these mixtures, once the copper damages the membrane, the antifungals can easily
548 enter the cell and exert their inhibitory effect. Regarding mixtures with Fe on B05.10, the
549 predominant effect was antagonistic, resulting in a decrease of the known individual efficacy of
550 each inhibitor, an opposite result than obtained for Cu-boscalid and Cu-fenhexamid. Then,
551 according to our results of membrane integrity, even though Fe showed a similar effect to Cu on
552 the cell membrane, a close result was expected, but in this case other additional interactions
553 could be possible modifying the inhibitory effect, enhancing the antagonistic effect. Concerning
554 wild strains, the predominant antagonistic effect with metal-fungicides mixture could be
555 correlated with the previous sensitivity and resistance pattern studied against iprodione, boscalid

556   and fenexhamid, and the cellular infrastructure or intraspecific differentiation developed in the
557   evolution of these wild strains and their genetic background. However, several additional studies
558   still are necessary to understand the interactions involved in this scenario.
559
560   Conidial germination of the B05.10 *B. cinerea* strain was likewise affected by the presence of
561   Cu, Fe, and Cu-Fe in liquid medium. For Cu_{50} and Cu_{50}-Fe_{50} at 6 h, the inhibition of conidial
562   germination did not show significant differences ($p = 0.9675$, 95%), while Fe_{50} had an inhibitory
563   effect slightly below them [$p = 0.5845$ (Fe vs. Cu); $p = 0.6313$ (Fe vs. Cu-Fe)]. According to
564   Judet-Correia et al. (2011), copper may bind to the surface of spores during germination. Thus, a
565   period of time is required for the detoxification process and selection of surviving spores. The
566   same authors reported that copper concentrations from 0-4 mM did not affect the lag time for the
567   growth of *B. cinerea*, suggesting that the germination did not depend on these copper
568   concentrations. In contrast, copper delayed the germination of spores at concentrations >4 mM,
569   needing more time to detoxify the medium by binding Cu at the surface of some spores. In our
570   case, the IC_{50} concentration of Cu was 2.78 mM. The toxic effects of Cu on the growth of other
571   fungi have also been reported (Jaworska et al., 1996; Tkaczuk, 2005), indicating that this
572   phenomenon could be dependent on the fungal species and physicochemical factors, as well as
573   metal concentration (Tobin, White & Gadd, 1994). Regarding the effect of iron, a relevant
574   inhibition of conidial germination was observed at 4 and 6 h, with a concentration of 9.08 mM
575   for Fe_{50} being calculated in this case. Fe^{2+} has been reported within a group of other tested
576   cations (Ca^{2+}, Mg^{2+}, K^+) where concentrations in the range of 0.001-1 mM did not influence
577   conidial germination (Nassr & Barakat, 2016). However, concentrations greater than 10 mM
578   resulted in an abrupt decrease in germination, especially for Fe^{2+}. It is likely that, before
579   germination, conidia are not altered at low cation concentrations in the growth substrate. Germ
580   tube growth becomes more sensitive to a wide range of cations (Ca^{2+}, Mg^{2+}, K^+, and Fe^{2+}). In
581   addition, Fe^{2+} seems to provide an important nutritional source for germ tube growth at low
582   concentrations (0.001 M), and it was found to support germ tube growth and elongation (Nassr
583   and Barakat, 2016). Lastly, the combination of Cu_{50}-Fe_{50} showed a toxic behavior on B05.10
584   germination dominated mainly by the effect of copper in the mixture.
585
586   Conidial germination was correlated with adhesion capacity for *B. cinerea* in the
587   presence of metallic inhibitors, which allowed us to evaluate this pathogen's ability to adhere to
588   environmental hosts (fruits, leaves, etc.), to advance in its proliferation and infection process.
589   The presence of copper in the medium resulted in the lowest adhesion capacity of the strain. Iron
590   and the mixture Cu-Fe showed an adhesion capacity 3.3-fold times higher than Cu, but without
591   statistically significant differences. This result could be attributable to Fe in the Cu-Fe mixture.
592   In the fungal adhesion process, biofilm formation was considered an important virulence
593   attribute of these pathogens (Fanning & Mitchell, 2012). Specifically, for *B. cinerea*, adhesion
594   was strongly related to the synthesis of glycoproteins in the outermost layer of the cell wall,
595   which act as 'stickers' on the host, facilitating propagation on the surface (Plaza et al., 2015).

596   Thus, a possible mechanism or effect of metallic inhibitors on adhesion could be related to an
597   inhibition of the synthesis of this type of protein. It is essential to consider the specific
598   mechanism of the fungal-host attachment process. Adhesion occurs at multiple stages of fungal
599   morphogenesis, where adhesion can be related to zoospores, conidia, germlings, hyphal
600   aggregates, and infection cushions (Epstein & Nicholson, 1997). Two specific stages have been
601   established in the adhesion of conidia and germlings in *B. cinerea*. The first stage occurred
602   immediately upon hydration of conidia, and was characterized by hydrophobic interaction forces.
603   The second stage of adhesion occurred after viable conidia had been incubated for several hours
604   under conditions that promoted germination. These asseverations were in line with the reported
605   correlation between adhesion and germination observed in *B. cinerea* (Doss et al., 1995; Torres-
606   Ossandón et al., 2019). The inhibitory effect on the germination of B05.10 shown by Fe, Cu, and
607   Cu-Fe can provide a key for understanding the actions observed in this study on the adhesion
608   capacity, where non-germinated conidia remained attached to the surface, as observed after the
609   aspiration process.
610

611   Cell membrane damage can result in loss of diffusible cellular solutes, oxidation of
612   membrane components, and increased permeability of the cell to external material (Cervantes &
613   Gutierrez-Corona, 1994; Tobin, White & Gadd, 1994). Our results suggest that metallic
614   inhibitors can affect the membrane integrity of B05.10. In this strain, when treated with Cu_{50},
615   Fe_{50}, or Cu_{50}-Fe_{50}, we observed a higher number of stained conidia in assays with PI. Comparing
616   the effect exerted by iron and copper on membrane integrity, a more significant number of
617   damaged conidia was observed with the individual presence of these metals. Exposure to high
618   Cu concentrations induced a disruption in membrane integrity, producing a selective change in
619   plasma membrane permeability, leading to loss of cell viability (Borkow & Gabbay, 2005;
620   Fleurat-Lessard et al., 2011). The equimolar mixture of metals exhibited a possible synergistic
621   effect on damage to the cell membranes of *B. cinerea*, compared to the effects of metal inhibitors
622   individually. Several approximations related to the copper fungitoxicity indicated that this metal
623   could damage membranes through various mechanisms, among which are redox imbalance at the
624   cellular level with damage to the membrane, delays in the germination of its spores, and
625   inhibitory effects on laccase activity, preventing infection (Buddhika, Savocchia & Steel, 2020;
626   Judet-Correia et al., 2011; Lamichhane et al., 2018). In the case of Fe, the total elucidation of its
627   antifungal mechanism has not been accomplished. It has been associated with an attack on
628   pathogens by induction of reactive oxygen species at the cellular level (Fleurat-Lessard et al.,
629   2011). In biological systems, where both copper and iron coexist, they can interact with oxygen
630   in their free unbound form by catalyzing the Fenton/Haber-Weiss reaction, which increases ROS
631   production. If cellular antioxidants cannot adequately counterbalance this production, the
632   oxidative damage of proteins, lipids and nucleic acids ensues (Letelier et al., 2010; Sharma et al.,
633   2012).
634

635   In fungi, the cell walls are fundamental for viability and pathogenicity, determining fungal
636 morphology, providing osmotic protection, and regulating material exchange with the
637 environment, adhesion to a substrate, or penetration (Cantu et al., 2009). Structurally, fungi cell
638 walls are composed of linear polymers of chitin, α-1,3; β-1,3- and β-1,6-glucans, and
639 mannoproteins (Adams, 2004). As has been shown, CFW preferentially binds to chitin in fungi
640 and interferes with cell wall assembly, while CR binds to β1,3-glucan and alters the assembly of
641 microfibrils at the cell wall (Ram & Klis, 2006). The wall is the first cellular site of interaction
642 with metal species and appears to have a major role in biosorption due to possession of numerous
643 uptake sites (Ghaed, Shirazi & Marandi, 2013; Tobin, White & Gadd, 1994). Our data suggest
644 that in the presence of CR or CFW plus metallic inhibitors (Cu_{50}, $Fe_{50,}$ and Cu_{50}-Fe_{50}), *B. cinerea*
645 showed non-statistically significant differences compared to the control strain without metal
646 treatment, indicating no major change in cell wall integrity. Chitin and chitosan are significant
647 metal-absorbing substances in cell walls of fungi (Ghaed, Shirazi & Marandi, 2013; Tobin,
648 White & Gadd, 1994; Volesky, 1990). Our data suggest that metal could be present in the cell
649 wall but would not alter the chitin and glucan contained in *B. cinerea*. However, additional
650 studies are required to corroborate these findings. For example, future studies can use HPLC
651 quantification of the β-glucans and chitin to compare the synthesis of polysaccharides with and
652 without metallic inhibitors.
653
654   Lastly, the study of the pathogenicity of *B. cinerea* in the presence of the metallic inhibitors
655 showed that copper and iron also affected virulence of *B. cinerea* on strawberries and tomato
656 leaves. Specifically, the strawberries senescence was observed to be lower for fruits inoculated
657 with copper compared to iron. However, in a host as tomato leaves the inhibition pattern was the
658 inverse of that observed in strawberry fruits, where iron inhibited *B. cinerea* more than copper
659 did. These differences can be analyzed from different points. Although copper and iron are
660 essential, an excess could result in the generation of ROS through the Fenton/Haber-Weiss
661 reaction and inactivation of enzymes by replacement of normal metal cofactors, thus affecting
662 the virulence mechanism (Gerwien et al., 2018). This could be associated with defects in
663 germination and membrane damage caused by copper and iron in these fungi as explained above.
664 Additionally, among the virulence factors, the ambient pH is considered the most important
665 physiochemical factor affecting cell growth, development, and the interaction host-*B. cinerea*
666 (Rascle et al., 2018). Hosts as the fruits typically exhibiting a pH ranging from 3.32 to 4.39,
667 whereas leaves, stems, and roots exhibit a higher pH ranging from 5.81 to 6.3 (Hua et al., 2018).
668 Precisely this case involves the typically acidic pH of fruits, where these metals are more
669 soluble, resulting in pH-dependent systems of metal homeostasis (Gerwien et al., 2018). This
670 suggests that pH may have played a role in the pathogenicity, however, more studies devoted to
671 the analysis of genes involved in iron and copper metabolism in *B. cinerea* are required,
672 considering the differences in inhibition patterns observed depending on the type of host using
673 the same metal concentration.
674

Conclusions

New insights are presented in this work for characterizing the inhibitory effect of Cu and Fe, separately and together, on *B. cinerea.* Our data shows that Cu and Fe can successfully inhibit the mycelial growth and conidial germination of *B. cinerea*, while tests of the Cu-Fe combination revealed that the inhibitory effect of Cu was dominant over Fe. The adhesion capacity of *B. cinerea* in the presence of the metallic inhibitors was correlated with the effect observed on conidial germination, where inhibited conidia continued to adhere to the surface. A negative effect exerted by metallic inhibitors on the plasma membrane integrity of *B. cinerea* was also observed. Our findings revealed that the cell wall was not altered by the antifungal effects of Cu, Fe, and Cu-Fe. However, future studies are required to corroborate these findings. Lastly, the pathogenicity test showed that the virulence level was controlled by the individual presence of Cu and Fe. The broad characterization developed in our work represents new contributions about the inhibitory effect of these metals on *B. cinerea* that can increase understanding of the mechanism involved at the cellular level and promote development of new metal-based fungicides to ensure sustainability of agri-food crops.

Acknowledgements

The authors would like to acknowledge the "Dirección de Investigación y Desarrollo (DIDULS-TTP212128 and TTP222122)" and the Doctoral Program from the University of La Serena-Chile for their support in the develop of this investigation. Also, we thank Dr(c) Matias Poblete for help us in the Fig S2, MSc. Bárbara Marambio-Alvarado and Lila Olivares-Urbina for their assistance in work at the Laboratory of Biochemistry and Molecular Biology, Department of Biology, University of La Serena, Chile.

References

Adams DJ. 2004. Fungal cell wall chitinases and glucanases. *Microbiology* 150, 2029–2035. https://doi.org/10.1099/mic.0.26980-0.

Antsotegi-Uskola M, Markina-Iñarrairaegui A, Ugalde U. 2020. New insights into copper homeostasis in filamentous fungi. *International Microbiology* 23, 65–73. https://doi.org/https://doi.org/10.1007/s10123-019-00081-5.

Balamurugan K & Schaffner W. 2006. Copper homeostasis in eukaryotes: Teetering on a tightrope. Biochimica et Biophysica Acta 1763, 737-746. https://doi.org/10.1016/j.bbamcr.2006.05.001

Biittner P, Koch F, Voigt K, Quidde T, Risch S, Blaich R, Briickner B, Tudzynski P. 1994. Variations in ploidy among isolates of *Botrytis cinerea*: implications for genetic and molecular analyses. *Current Genetics* 25, 445–450. https://doi.org/10.1007/BF00351784.

Blatzer M & Latgé J. 2017. Metal-homeostasis in the pathobiology of the opportunistic human fungal pathogen *Aspergillus fumigatus*. *Current Opinion in Microbiology* 40, 152–159. https://doi.org/10.1016/j.mib.2017.11.015.

Borkow G, Gabbay J. 2005. Copper as a Biocidal Tool. *Current Medicinal Chemistry* 12, 2163–2175. https://doi.org/10.2174/0929867054637617.

Buddhika UVA, Savocchia S, Steel CC. 2020. Copper induces transcription of BcLCC2 laccase gene in phytopathogenic fungus, *Botrytis cinerea*. *Mycology* 12, 48–57. https://doi.org/10.1080/21501203.2020.1725677.

Cantu D, Greve LC, Labavitch JM, Powell ALT. 2009. Characterization of the cell wall of the ubiquitous plant pathogen *Botrytis cinerea*. *Mycological Research* 113, 1396–1403. https://doi.org/10.1016/j.mycres.2009.09.006.

Castro P, Mendoza L, Vásquez C, Cornejo P, Navarro F, Lizama K, Santander R, Cotoras M. 2019. Antifungal Activity against *Botrytis cinerea* of 2,6-Dimethoxy-4-(phenylimino) cyclohexa-2,5-dienone Derivatives. *Molecules* 24. https://doi.org/10.3390/molecules24040706.

Cervantes C & Gutierrez-Corona F. 1994. Copper resistance mechanisms in bacteria and fungi. *FEMS Microbiology Reviews* 14, 121–137. https://doi.org/10.1111/j.1574-6976.1994.tb00083.x.

751 Cherrad S, Charnay A, Hernandez C, Steva H, Belbahri L. 2018. Emergence of boscalid-resistant
752 strains of *Erysiphe necator* in French vineyards. *Microbiological Research* 216, 79–84.
753 https://doi.org/10.1016/j.micres.2018.08.007.
754
755 Cheung N, Tian L, Liu X, Li X. 2020. The Destructive Fungal Pathogen *Botrytis cinerea* —
756 Insights from Genes Studied with Mutans Analysis. *Pathogens* 9, 1–46.
757 https://doi.org/10.3390/pathogens9110923.
758
759 Choquer M, Fournier E, Kunz C, Levis C, Pradier J, Simon A, Viaud M. 2007. *Botrytis cinerea*
760 virulence factors: new insights into a necrotrophic and polyphageous pathogen. *FEMS*
761 *Microbiology Letters* 277, 1–10. https://doi.org/10.1111/j.1574-6968.2007.00930.x.
762
763 Condon BJ, Oide S, Gibson DM, Krasnoff SB, Turgeon BG. 2014. Reductive Iron Assimilation
764 and Intracellular Siderophores Assist Extracellular Siderophore-Driven Iron Homeostasis and
765 Virulence. *MPMI* 27, 793–808.
766
767 Davies CR, Wohlgemuth F, Young T, Violet J, Dickinson M, Sanders J, Vallieres C, Avery SV.
768 2021. Evolving challenges and strategies for fungal control in the food supply chain. *Fungal*
769 *Biology Reviews* 36, 15–26. https://doi.org/10.1016/j.fbr.2021.01.003.
770
771 Dean R, Kan J, Pretorius ZA, Hammond-Kosack K, Pietro A, Di Spanu PD, Rudd JJ, Dickman
772 M, Kahmann R, Ellis J, Foster GD. 2012. The Top 10 fungal pathogens in molecular plant
773 pathology. *Molecular Plant Pathology*. 13, 414–430. https://doi.org/10.1111/J.1364-
774 3703.2011.00783.X.
775
776 Debieu D, Bach J, Montesinos E, Fillinger S, Leroux P. 2013. Role of sterol 3-ketoreductase
777 sensitivity in susceptibility to the fungicide fenhexamid in *Botrytis cinerea* and other
778 phytopathogenic fungi. *Pest Management Science* 69, 642–651. https://doi.org/10.1002/ps.3418.
779
780 Doss RP, Potter SW, Soeldner AH, Christian JK, Fukunaga LE. 1995. Adhesion of germlings of
781 *Botrytis cinerea*. *Applied and Environmental Microbiology* 61, 260–265.
782 https://doi.org/10.1128/aem.61.1.260-265.1995.
783
784 Epstein L & Nicholson R. 1997. Adhesion of Spores and Hyphae to Plant Surfaces, in: The
785 Mycota (A Comprehensive Treatise on Fungi as Experimental Systems for Basic and Applied
786 Research). Springer, Berlin, pp. 11–22. https://doi.org/10.1007/978-3-662-10370-8_2.
787
788 Fanning S & Mitchell AP. 2012. Fungal Biofilms. *PLos Pathogens* 8, 1–4.
789 https://doi.org/10.1371/journal.ppat.1002585.
790

791 Fleurat-Lessard P, Dédaldéchamp F, Thibault F, Béré E, Roblin G. 2011. Antifungal effects of
792 iron sulfate on grapevine fungal pathogens. *Scientia Horticulturae* (Amsterdam). 130, 517–523.
793 https://doi.org/10.1016/j.scienta.2011.07.004.
794
795 Gerwien F, Skrahina V, Kasper L, Hube B, Brunke S. 2018. Metals in fungal virulence. *FEMS*
796 *Microbiology Reviews* 42, 1–21. https://doi.org/10.1093/femsre/fux050.
797
798 Ghaed S, Shirazi EK, Marandi R. 2013. Biosorption of Copper Ions by Bacillus and Aspergillus
799 Species. *Adsorption Science & Technology*. 3, 869–890. https://doi.org/10.1260/0263-
800 6174.31.10.869.
801
802 Giovagnoli-Vicuña C, Briones-Labarca V, Pizarro S, Delgadillo A. 2019. A Square Wave
803 Voltammetry Study on the Antioxidant Interaction and Effect of Extraction Method for Binary
804 Fruit Mixture Extracts. *Journal of Chemistry*, (ID 8706061). https://doi.org/10.1155/2019/8706061
805
806 Giraud T, Fortini D, Levis C, Lamarque C, Leroux P, Lobuglio K, Brygoo Y. 1999. Two Sibling
807 Species of the *Botrytis cinerea* Complex, transposa and vacuma, Are Found in Sympatry on
808 Numerous Host Plants. Ecology & *Population Biology* 89, 967–973.
809
810 Greenshields DL, Liu G, Wei Y. 2007. Roles of Iron in Plant Defense and Fungal Virulence.
811 *Plant Signaling & Behavior*. 2, 300–302. https://doi.org/10.1242/jcs.001362.
812
813 Haas H, Eisendle M, Turgeon BG. 2008. Siderophores in Fungal Physiology and Virulence.
814 *Annual Review of Phytopathology* 46, 149–87.
815 https://doi.org/10.1146/annurev.phyto.45.062806.094338.
816
817 Haas H. 2014. Fungal siderophore metabolism with a focus on *Aspergillus fumigatus*. *Natural*
818 *Products Reports*, *31*, 1266. DOI: 10.1039/c4np00071d
819
820 Haas H, Eisendle M, Turgeon G. 2008. Siderophores in Fungal Physiology and Virulence. *Annu.*
821 *Rev. Phytopathol* 46:149–87. https://doi.org/10.1146/annurev.phyto.45.062806.094338
822
823 Hernández-Monjaraz WS, Caudillo-Pérez C, Salazar-Sánchez PU, Macías-Sánchez KL. 2018.
824 Fungal and Bacterial Physiology Influence of iron and copper on the activity of laccases in
825 *Fusarium oxysporum f.* sp. *lycopersici*. *Brazilian Journal of Microbiol*ogy 49, 269–275.
826 https://doi.org/10.1016/j.bjm.2018.06.002.
827
828 Hua L, Yong C, Zhanquan Z, Boqiang L, Guozheng Q, Shiping T. 2018. Pathogenic mechanisms
829 and control strategies of *Botrytis cinerea* causing post-harvest decay in fruits and vegetables.
830 *Food Quality and Safety*. 3, 111–119. https://doi.org/10.1093/fqsafe/fyy016.

831

832 Imlay JA. 2014. The Mismetallation of Enzymes During Oxidative Stress. *Journal of Biological*
833 *Chemistry* 41, 28121–8. https://doi.org/10.1074/jbc.R114.588814.

834

835 Irving H, Williams RJP. 1948. Order of Stability of Metal Complexes. *Nature* 162, 746–747.
836 https://doi.org/https://doi.org/10.1038/162746a0.

837

838 Jaworska M, Radkowska A, Ropek D, Tomasik P. 1996. Effect of metal ions on *Paecilomyces*
839 *fumosoroseus*. *IOBC/WPRS Bull* 19, 221.

840

841 Jhonson L. 2008. Iron and siderophores in fungal-host interactions. *Mycological Research* 112,
842 2, 170-183. https://doi.org/10.1016/j.mycres.2007.11.012

843

844 Judet-Correia D, Charpentier C, Bensoussan M, Dantigny P. 2011. Modelling the inhibitory
845 effect of copper sulfate on the growth of *Penicillium expansum* and *Botrytis cinerea*. *Letters in*
846 *Applied Microbiology*. 53, 558–564. https://doi.org/10.1111/j.1472-765X.2011.03149.x.

847

848 Kai K, Hua C, Sui Y, Bi W, Shi W, Zhang D, Ye Y. 2020. Curcumin triggers the immunity
849 response in kiwifruit against *Botrytis cinerea*. *Scientia Horticulturae* (Amsterdam). 274, 109685.
850 https://doi.org/10.1016/j.scienta.2020.109685.

851

852 Konetschny-Rapp S, Jung G, Huschka HG, Winkelmann, G. 1988. Isolation and identification of
853 the principal siderophore of the plant pathogenic fungus *Botrytis cinerea*. *Biology of Metals*, *1*,
854 90–98. https://doi.org/10.1007/BF01138066

855

856 Kumar S, Stecher G, Li M, Knyaz C, Tamura K. 2018. MEGA X: Molecular Evolutionary
857 Genetics Analysis across Computing Platforms. *Molecular Biology and Evolution*. 35, 1547–
858 1549. https://doi.org/10.1093/molbev/msy096.

859

860 Lamichhane JR, Osdaghi E, Behlau F, Köhl, J, Jones JB, Aubertot J. 2018. Thirteen decades of
861 antimicrobial copper compounds applied in agriculture. A review. *Agronomy for Sustainable*
862 *Development* 38. https://doi.org//10.1007/s13593-018-0503-9.

863

864 Leiva-Portilla DJ, Rodríguez-Nuñez KE, Rodríguez-Ramos FJ, Delgadillo Acevedo A, Uribe, E.
865 2020. Impact on Physicochemical Composition and Antioxidant Activity of the Wild Edible
866 Mushroom *Cyttaria espinosae* Subjected to Drying. Chemistry & Biodiversity 17, 20.
867 https://doi.org/10.1002/cbdv.202000642

868

869 Letelier ME, Sánchez-Jofré S, Peredo-Silva L, Cortés-Troncoso J, Aracena-Parks P. 2010.
870 Mechanisms underlying iron and copper ions toxicity in biological systems: Pro-oxidant activity

871 and protein-binding effects. *Chemical-Biological Interactions* 188, 220–227.
872 https://doi.org/10.1016/j.cbi.2010.06.013.

874 Li M, Wang S, Tian Z, Li S, Chen Y, Jia Z, Liu K, Zhao A. 2019. Effects of foliar application of
875 the mixture of copper and chelated iron on the yield, quality, photosynthesis, and microelement
876 concentration of table grape (*Vitis vinifera L.*). *Sciencia Horticulturae. 254*, 106–115.
877 https://doi.org/10.1016/j.scienta.2019.04.075

879 Liu Y, Kong D, Wu HL, Ling HQ. 2020. Iron in Plant-pathogen Interactions. *Journal of*
880 *Experimental Botany* 72, 2114–2124. https://doi.org/https://doi.org/10.1093/jxb/eraa516.

882 Ma J, Zhang M, Liu Z, Chen H, Li Y, Sun Y, Ma Q, Zhao C. 2019. Effects of foliar application
883 of the mixture of copper and chelated iron on the yield, quality, photosynthesis, and
884 microelement concentration of table grape (*Vitis vinifera* L.). *Scientia Horticulturae* 254, 106-
885 115. https://doi.org/10.1016/j.scienta.2019.04.075

887 Misslinger M, Hortschansky P, Brakhage AA, Haas H. 2021. Fungal iron homeostasis with a
888 focus on *Aspergillus fumigatus*. *BBA - Molecular Cell Research.* 1868.
889 https://doi.org/10.1016/j.bbamcr.2020.118885.

891 Muñoz C, Gómez-Talquenca S, Oriolani E, Combina M. 2010. Genetic characterization of
892 grapevine-infecting *Botrytis cinerea* isolates from Argentina. *Revista Iberoamericana de*
893 *Micología* 27, 66–70. https://doi.org/10.1016/j.riam.2009.12.006.

895 Nakajima M & Akutsu K. 2014. Virulence factors of *Botrytis cinerea*. *Journal of General Plant*
896 *Pathology* 80, 15–23. https://doi.org/10.1007/s10327-013-0492-0.

898 Nassr S & Barakat R. 2016. Effect of Factors on Conidium Germination of *Botrytis cinerea* in
899 vitro. *International Journal of Plant & Soil Science* 2, 41–54.
900 https://doi.org/10.9734/IJPSS/2013/2772.

902 Notte AM, Plaza V, Marambio-Alvarado B, Olivares-Urbina L, Poblete-Morales M, Silva-
903 Moreno E, Castillo L. 2021. Molecular identification and characterization of *Botrytis cinerea*
904 associated to the endemic flora of semi-desert climate in Chile. *Current Research in Microbial*
905 *Sciences* 2. https://doi.org/10.1016/j.crmicr.2021.100049.

907 Olea F, Bravo A, Mart R, Thomas M, Sedan C, Espinoza L, Zambrano E, Carvajal D, Silva-
908 Moreno E, Carrasco H. 2019. Antifungal Activity of Eugenol Derivatives against *Botrytis*
909 *cinerea*. *Molecules* 24, 1–14. https://doi.org/10.3390/molecules24071239.
910

911 Pappas A, Fisher D. 1979. A comparison of the mechanism of action of vinclozolin,
912 procymidone, iprodione, and prochloraz against *Botrytis cinerea*. *Pesticides Science*. 10: 239–
913 246. https://doi.org/10.1002/ps.2780100308
914
915 Pinedo C, Wang C, Pradier J, Dalmais B, Pêcheur P, Le Morgant, G Collado IG, Cane DE,
916 Viaud M. 2009. The Sesquiterpene Synthase from the Botrydial Biosynthetic Gene Cluster of the
917 Phytopathogen *Botrytis cinerea*. *ACS Chemical Biology* 3, 791–801.
918 https://doi.org/10.1021/cb800225v.
919
920 Piqueras C, Latorre B, Torres R. 2014. Effectiveness of isofetamid, a new succinate
921 dehydrogenase inhibitor fungicide, in the control of grapevine gray mold. *Ciencia e
922 Investigación Agraria*. 41(3):365-374. https://doi.org/10.4067/s0718-16202014000300009.
923
924 Plaza V, Lagües Y, Carvajal M, Pérez-García LA, Mora-Montes HM, Canessa P, Larrondo LF,
925 Castillo L. 2015. bcpmr1 encodes a P-type Ca 2 + / Mn 2 + -ATPase mediating cell-wall
926 integrity and virulence in the phytopathogen *Botrytis cinerea*. *Fungal Genetics and Biology*. 76,
927 36–46. https://doi.org/10.1016/j.fgb.2015.01.012.
928
929 Plesken C, Pattar P, Reiss B, Noor ZN, Zhang L, Klug K, Huettel B, Hahn M. 2021. Genetic
930 Diversity of *Botrytis cinerea* Revealed by Multilocus Sequencing, and Identification of *B.
931 cinerea* Populations Showing Genetic Isolation and Distinct Host Adaptation. *Frontiers in Plant
932 Science*. 12, 1–15. https://doi.org/10.3389/fpls.2021.663027.
933
934 Quidde T, Osbourn A, Tudzynski P. 1998. Detoxification of α -tomatine by *Botrytis cinerea*.
935 *Physiology and Molecular Plant Pathology*. 151–165. https://doi.org/10.1006/pmpp.1998.0142.
936
937 Ram AFJ & Klis FM. 2006. Identification of fungal cell wall mutants using susceptibility assays
938 based on Calcofluor white and Congo red. *Nature Protocols* 1, 2253–2256.
939 https://doi.org/10.1038/nprot.2006.397.
940
941 Rascle C, Dieryckx C, Dupuy JW, Muszkieta L, Droux M, Bruel C, Girard V, Poussereau N. 2018.
942 The pH regulator PacC: A host-dependent virulence factor in *Botrytis cinerea*. *Environmental
943 Microbiology Reports*, *10*(5). https://doi.org/10.1111/1758-2229.12663
944 Robinson JR, Isikhuemhen OS, Anike FN. 2021. Fungal – Metal Interactions: A Review of
945 Toxicity and Homeostasis. *Journal of Fungi* 7, 1–30.
946 https://doi.org/https://doi.org/10.3390/jof7030225.
947
948 Rout GR & Sahoo S. 2015. Role of iron in plant growth and metabolism. *Reviews in Agricultural
949 Science*, *3*, 1–24. https://doi.org/10.7831/ras.3.1
950

951 Rupp S, Weber RWS, Rieger D, Detzel P, Hahn M. 2017. Spread of *Botrytis cinerea* Strains with
952 Multiple Fungicide Resistance in German Horticulture. *Frontiers in Microbiology*. 7, 1–12.
953 https://doi.org/10.3389/fmicb.2016.02075

955 Saitoh Y, Izumitsu K, Morita A, Tanaka C. 2010. A copper-transporting ATPase BcCCC2 is
956 necessary for pathogenicity of *Botrytis cinerea*. *Molecular Genetics and Genomics* 284, 33–43.
957 https://doi.org/10.1007/s00438-010-0545-4

959 Saitou N & Nei M. 1987. The neighbor-joining method: a new method for reconstructing
960 phylogenetic trees. *Molecular Biology and Evolution* 4, 406–425.
961 10.1093/oxfordjournals.molbev.a040454

963 Sambrook J, Fritsch EF, Maniatis T. 1989. Molecular Cloning: A Laboratory Manual. Cold
964 Spring Harbor Laboratory Press.

966 Schouten A, Wagemakers L, Stefanato FL, Kaaij RM, Van Der Kan, JAL. 2002. Resveratrol acts
967 as a natural profungicide and induces self-intoxication by a specific laccase. *Molecular*
968 *Microbiology* 43, 883–894. 10.1046/j.1365-2958.2002.02801.x

970 Sharma P, Jha AB, Dubey RS, Pessarakli M. 2012. Reactive Oxygen Species, Oxidative
971 Damage, and Antioxidative Defense Mechanism in Plants under Stressful Conditions. *Journal of*
972 *Botany* 2012, 26. https://doi.org/10.1155/2012/217037

974 Siewers V, Viaud M, Jimenez-Teja D, Collado IG, Gronover CS, Pradier J, Tudzynski B,
975 Tudzynski P, Botanik I, Münster WW, Münster D, De U. 2005. Functional analysis of the
976 cytochrome P450 monooxygenase gene bcbot1 of *Botrytis cinerea* indicates that Botrydial is a
977 strain-specific virulence factor. *Molecular. Plant-Microbe Interactions* 18, 602–612.
978 10.1094/MPMI-18-0602

980 Smith AD, Logeman BL, Thiele DJ. 2017. Copper Acquisition and Utilization in Fungi. *Annual*
981 *Review of Microbiology*. 71, 597–623. https://doi.org/10.1146/annurev-micro-030117- 020444.

983 Spada M, Pugliesi C, Fambrini M, Pecchia S. 2021. Silencing of the Slt2-Type MAP Kinase
984 Bmp3 in *Botrytis cinerea* by Application of Exogenous dsRNA Affects Fungal Growth and
985 Virulence on Lactuca sativa. *International Journal of Molecular Science* 22.
986 10.3390/ijms22105362

988 Staats M, Baarlen P, Van Kan, J.A.L. 2005. Molecular Phylogeny of the Plant Pathogenic Genus
989 Botrytis and the Evolution of Host Specificity. *Molecular Biology and Evolution* 22.
990 https://doi.org/10.1093/molbev/msi020.

991

992 Thompson JD, Higgins DG, Gibson T. 1994. CLUSTAL W: improving the sensitivity of
993 progressive multiple sequence alignment through sequence weighting, position-specific gap
994 penalties and weight matrix choice. *Nucleic Acids Research.* 22, 4673–4680.
995 10.1093/nar/22.22.4673

996

997 Tkaczuk C. 2005. The Effect of Selected Heavy Metal Ions on the Growth and Conidial
998 Germination of the Aphid Pathogenic Fungus *Pandora neoaphidis* (Remaudiére et Hennebert)
999 Humber. *Polish Journal of Environmental Studies.* 14, 897–902.

1000

1001 Tobin JM, White C, Gadd GM. 1994. Metal accumulation by fungi: applications in
1002 environmental biotechnology. *Journal of Industrial Microbiology.* 13, 126–130.
1003 https://doi.org/10.1007/BF01584110

1004

1005 Torres-Ossandón MJ, Vega-Gálvez A, Salas CE, Rubio J, Silva-Moreno E, Castillo L. 2019.
1006 Antifungal activity of proteolytic fraction (P1G10) from (*Vasconcellea cundinamarcensis*) latex
1007 inhibit cell growth and cell wall integrity in *Botrytis cinerea. International Journal of Food*
1008 *Microbioly.* 289, 7–16. https://doi.org/10.1016/j.ijfoodmicro.2018.08.027.

1009

1010 Touati D. 2000. Iron and Oxidative Stress in Bacteria. *Archives of Biochemistry and Biophysics,*
1011 *373*(1), 1–6. DOI: 10.1006/abbi.1999.1518

1012

1013 Vasquez-Montaño E, Hoppe G, Vega A, Olivares-Yañez C. 2020. Defects in the Ferroxidase
1014 That Participates in the Reductive Iron Assimilation System Results in Hypervirulence in
1015 *Botrytis cinerea. mBio* 11, 1–20. https://doi.org/https://doi.org/10.1128/mBio .01379-20.

1016

1017 Volesky B. 1990. Removal and recovery of heavy metals by biosorption., in: Biosorption of
1018 Heavy Metals. CRC Press, Boca Ratón, Florida, US, p. 408.

1019

1020 White T, Bruns T, Lee S, Taylor J, Innis M, Gelfand DS. 1990. Amplification and Direct
1021 Sequencing of Fungal Ribosomal RNA Genes for Phylogenetics, in: PCR Protocols. Academic
1022 Press, Inc.

1023

1024 Zoroddu MA, Zanetti S, Pogni R, Basosi R, Dipartimento MAZ, Sassari U. 1996. An Electron
1025 Spin Resonance Study and Antimicrobial Activity of Copper (II) -Phenanthroline Complexes.
1026 *Journal of Inorganic Biochemistry.* 63, 291–300.

1027

Figure 1

Effect of metallic inhibitors on the growth of *B. cinerea* in solid media.

Mycelial growth inhibition behavior during seven days of incubation at different concentrations, and the effect on mycelial growth at day 7 of incubation: Cu (A) and Fe (B). Data represent means ± SD from six independent experiments.

A
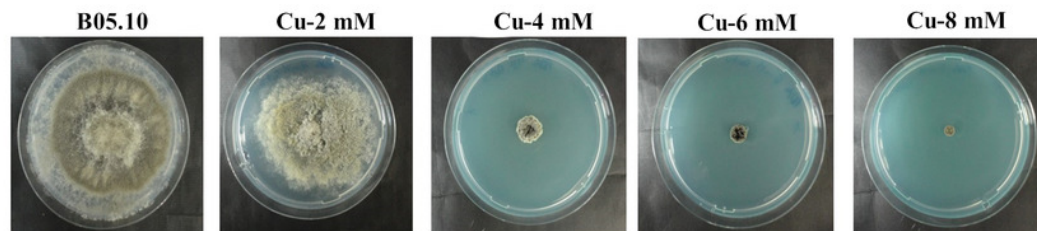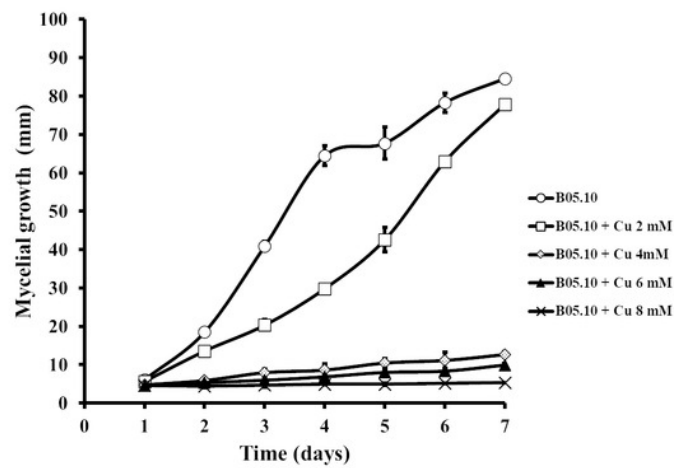
B
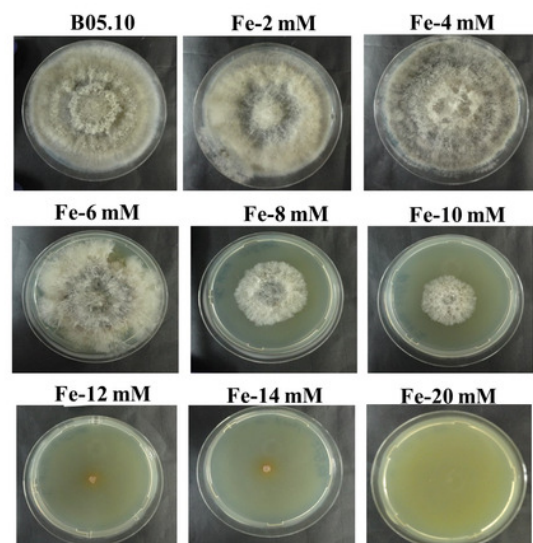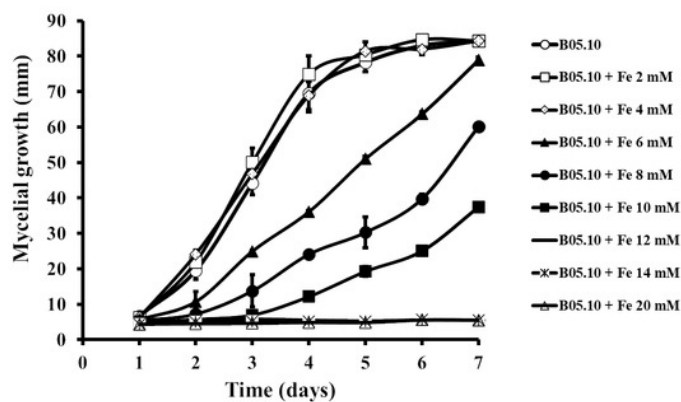
Figure 2

Effect of Cu-Fe equimolar mixture on the growth of *B. cinerea* in solid media

(A) Mycelial growth inhibition behavior during seven days of incubation at different concentrations, and (B) effect on mycelial growth at day 7 of incubation. Data represent means ± SD from six independent experiments.
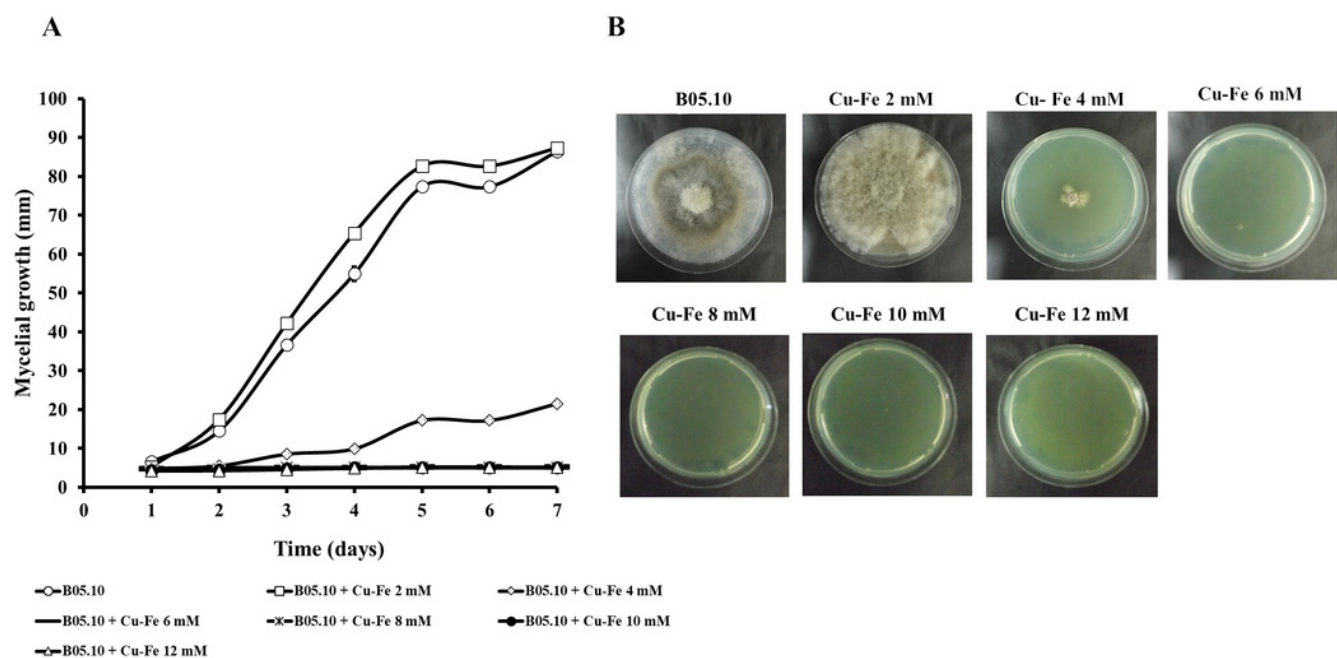
Figure 3

Effect of Fe_{50} (9.08 mM), Cu_{50} (2.87 mM), and Cu_{50}-Fe_{50} on mycelial growth of different wild strains of *B. cinerea.*

Data represent means ± SD from six independent experiments.
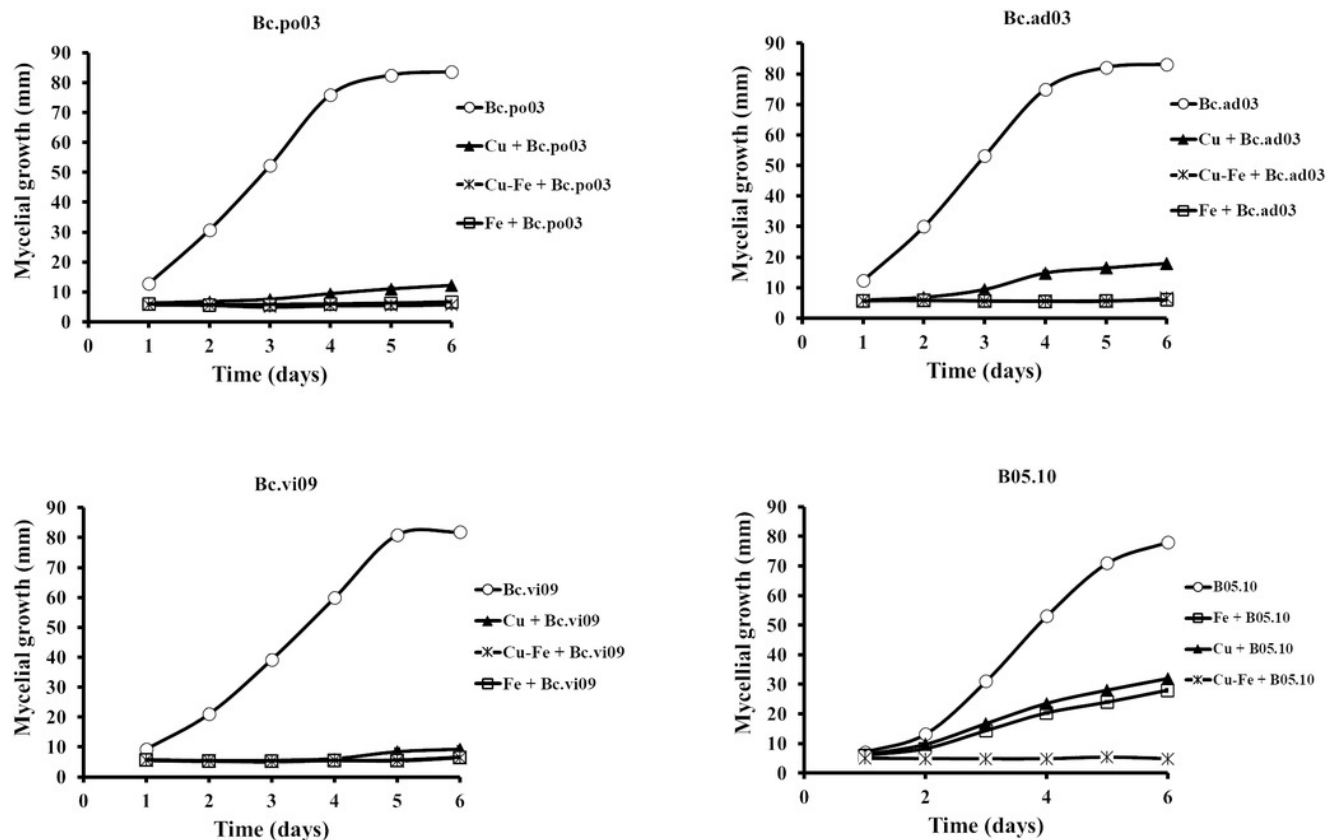
Figure 4

Effect of Fe_{50} (9.08mM), Cu_{50} (2.87 mM), and Cu_{50}-Fe_{50} on conidial germination of *B. cinerea.*

(A) Percentage of germination inhibition and (B) Images (40x magnification, scale bar 10 µm) of germinated conidia at different times and metallic inhibitors. Data represent means ± SD from six independent experiments.

A
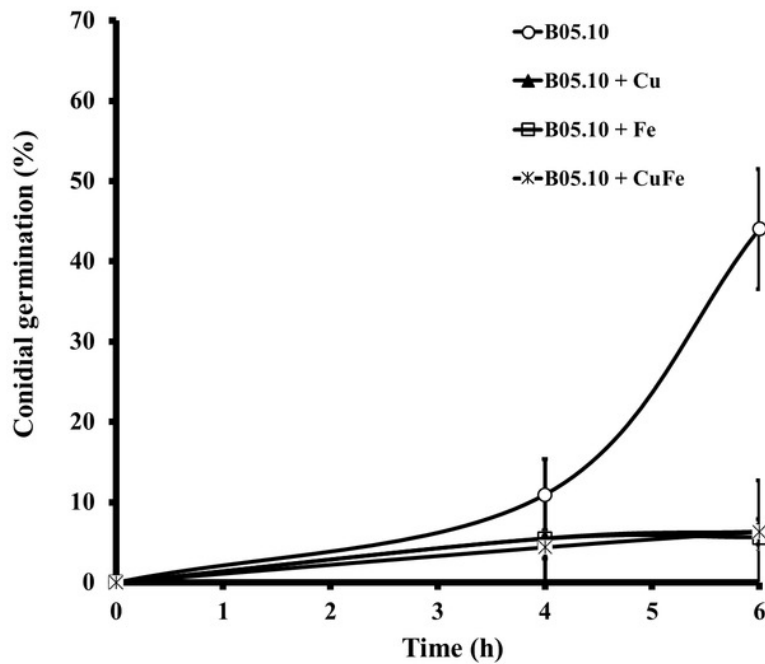
B
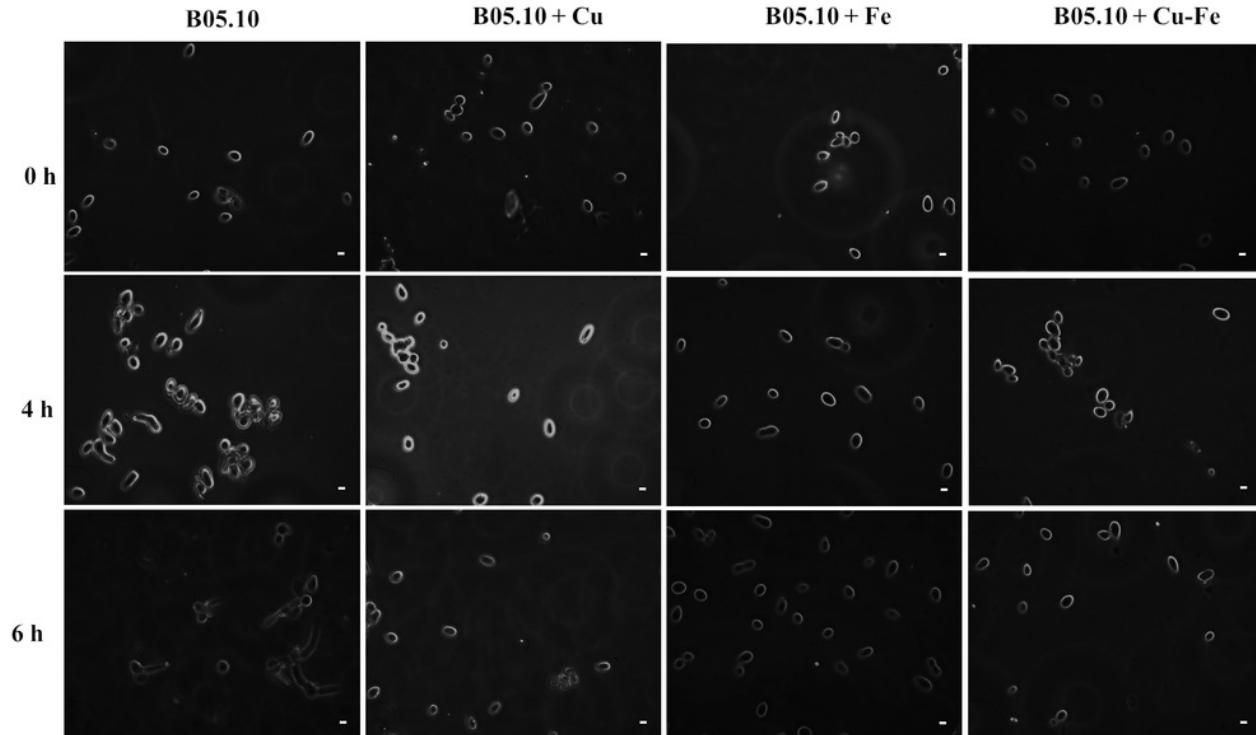
40× magnification, scale bar 10μm

Figure 5

Effect of Cu_{50} (2.87 mM), Fe_{50} (9.08mM), and Cu_{50}-Fe_{50} on adhesion capacity of *B. cinerea.*

(A) and (B): percent inhibition of metallic inhibitors on the adhesion and biofilm formation, and bound mycelia stained with crystal violet and visualized by fluorescence microscopy (10× magnification, scale bar = 10µm). All experiments were performed three times with n = 6. Different letters indicate significant differences ($p < 0.05$).
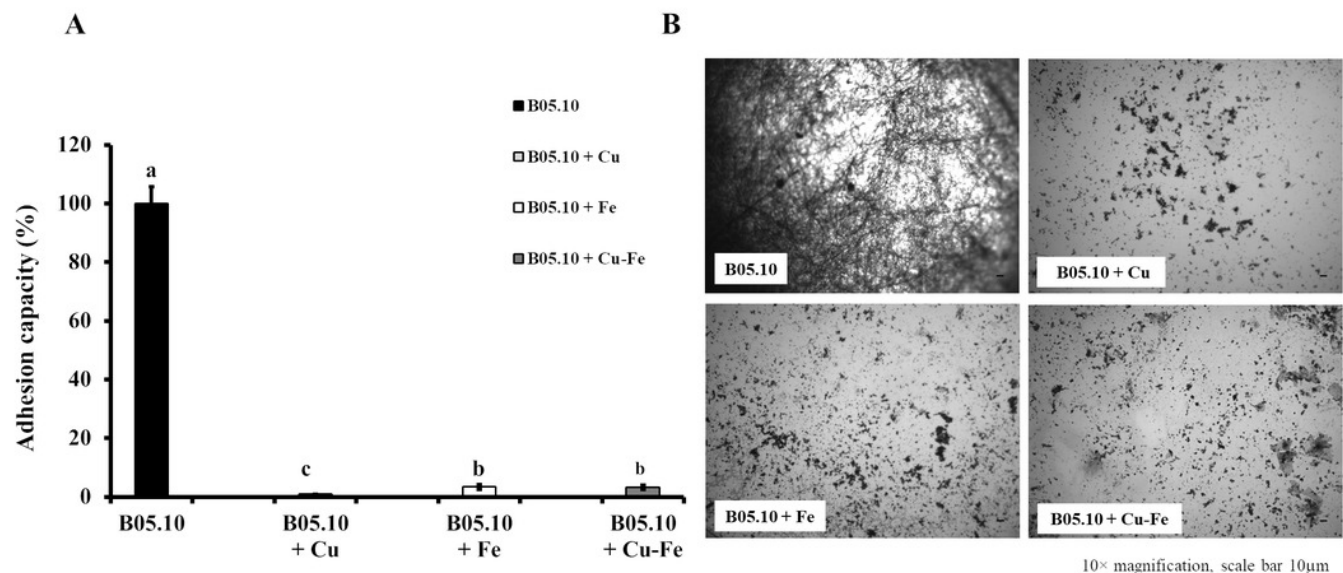
Figure 6

Effect of the metals and Congo red on the cell wall in *B. cinerea*

Sensitivity of B05.10 growth with or without Fe_{50} (9.08mM), Cu_{50} (2.87 mM), and Cu_{50}-Fe_{50} in solid media with Congo red (CR). Data represent means ± SD from nine independent experiments.
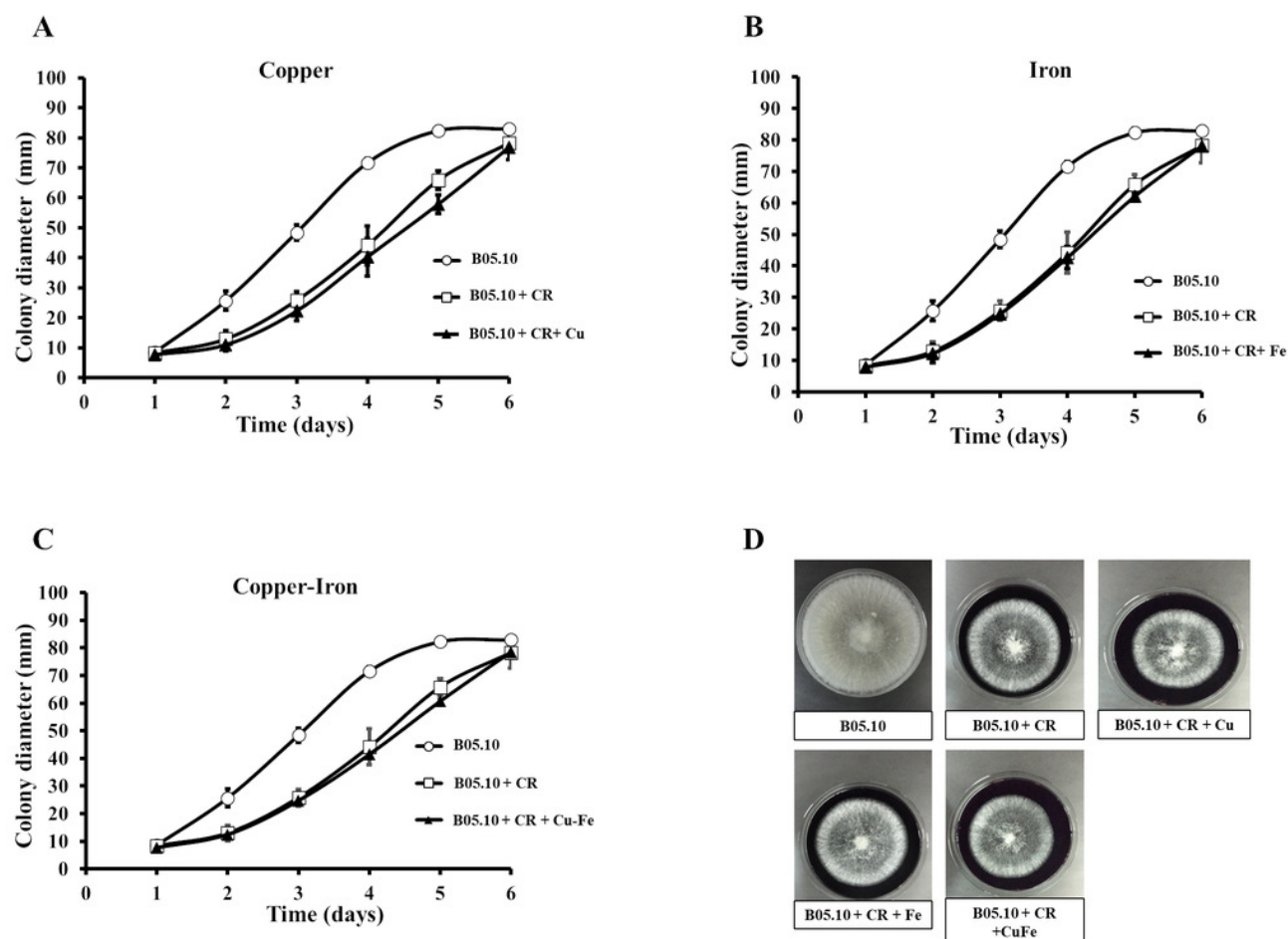
Figure 7

Effect of the metals and Calcofluor white on the cell wall in *B. cinerea*

Sensitivity of B05.10 with or without Fe_{50} (9.08mM), Cu_{50} (2.87 mM), and Cu_{50}-Fe_{50} grown on solid media with calcofluor white (CFW). Data represent means ± SD from nine independent experiments.
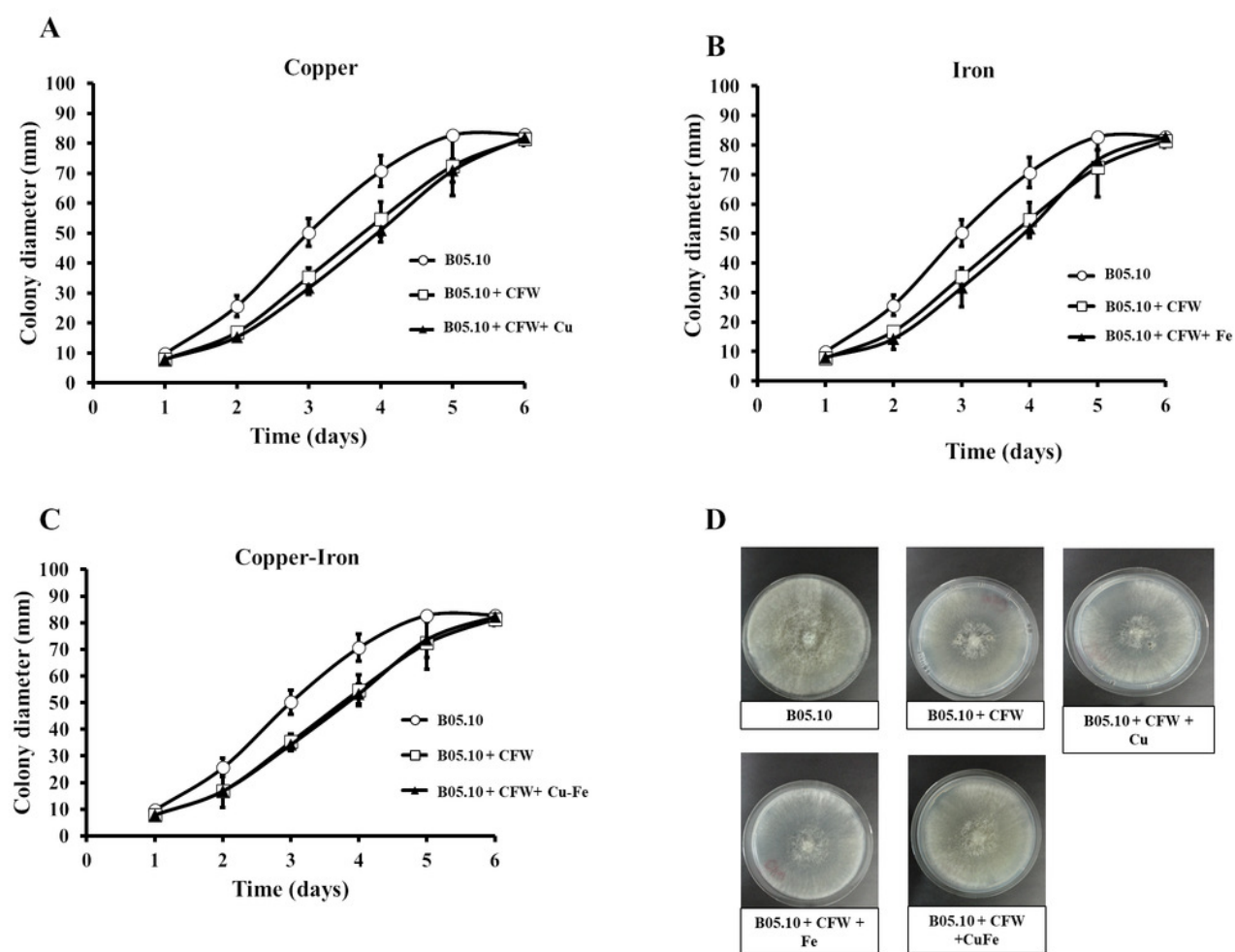
Figure 8

Effect of the metals on plasma membrane integrity of *B. cinerea*.

(A) Effect of Fe_{50} (9.08mM), Cu_{50} (2.87 mM), and Cu_{50}-Fe_{50} on membrane integrity of *B. cinerea*.

(B) effect on *B. cinerea* cells treated with PI (40x magnification, scale bar = 10 μm). Data

represent means ± SD from six independent experiments.
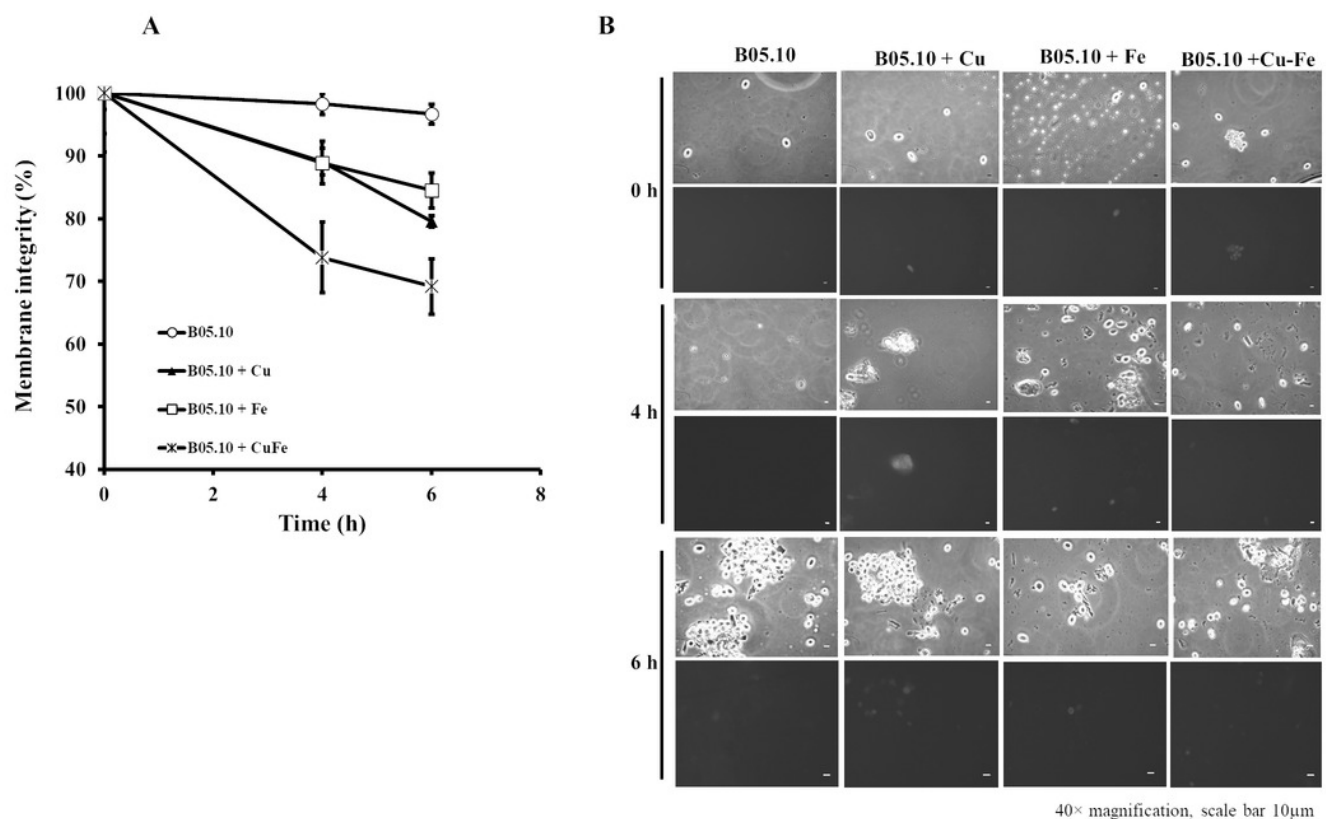
Figure 9

Pathogenicity assay of the *Botrytis* B05.10 strain in presence of metallic inhibitors.

(A) and (B) Pathogenicity test carried out for B05.10 (2.5×10^5 conidia/mL) in the presence of Fe_{50} (9.08mM), and Cu_{50} (2.87 mM) placed inside wounded strawberry fruits, with comparisons at days 0 and 4. Data represent means $\pm$ SD from 15 independent experiments. (C) and (D) Droplets of 5 ml containing 2.5×10^5 conidia/ml for B05.10 in the presence of Fe_{50} (9.08mM), and Cu_{50} (2.87 mM) placed onto the surface of a tomato leaf. Lesion development was scored after four dpi. Data represent means $\pm$ SD from 10 independent experiments.

A

B

C

D